

1 **Salt-marsh areas as copper complexing ligand sources to estuarine and coastal systems**

2 Juan SANTOS-ECHEANDÍA^{a,b,*}, Miguel CAETANO^a, Luis M. LAGLERA^c, Carlos VALE^a

3 ^a IPMA, Portuguese Institute of Sea and Atmosphere, Avenida Brasília 1446-006 Lisboa, Portugal

4 ^b Marine Biogeochemistry Group. Instituto de Investigaciones Marinas (CSIC). Vigo (Spain)

5 ^c University of Balearic Islands, Chemistry Department, Spain

6 *Corresponding author: jusae@iim.csic.es; tel. (+34) 986231930; fax(+34)986292762.

7 **Abstract**

8 Dissolved copper levels, copper complexing capacities and conditional stability constants have been
9 determined in the Tagus estuarine waters and one of the saltmarshes located in this estuary, the
10 Rosario saltmarsh. Tagus estuarine waters show a constant and around 20 nM copper concentration
11 during the estuarine mixing. Most of this copper is organically complexed by a strong ligand (L₁) with a
12 concentration that varies between 19-55 nM and a log K' between 14.14-15.75. In addition L₁/Cu ratios
13 are quite constants and close to 1 all through the estuary, indicating the same source. A second and
14 weakest ligand (L₂) was also detected in these waters in higher concentrations (36-368 nM) but with a
15 lower log K' that varies between 12.06-13.13. The present work has demonstrated that salt-marsh areas
16 are important and continuous sources of copper complexing ligands to the Tagus estuary. Noticeable,
17 tidal induced transport continuously feed these waters with copper and ligands, mainly with the
18 strongest one. This continuous input, together with the high residence times of this system results in a
19 quite constant concentration along the salinity gradient. This input represents 95% of the ligand present
20 in the estuary.

21 **Keywords:** copper; ligands; speciation; estuary; salt-marsh; Tagus

22 **1. INTRODUCTION**

23 Salt-marshes are among the most common and extensive intertidal habitats along temperate coastlines.
24 Several studies have shown that salt marshes incorporate large quantities of anthropogenic metals into
25 the colonized sediments (Caçador et al., 1993; Sundby et al., 1998; Caetano et al., 2007). Root-sediment

26 interactions appear to contribute to the metal enrichment of colonized sediments and belowground
27 biomass (Caçador et al., 1993) as well as porewaters (Santos-Echeandía et al., 2010).

28 Not only the concentrations, but also trace metals chemical forms in estuarine water (porewater and
29 water column) may control their bioavailability and toxicity. In the water column, speciation of many
30 biologically active trace metals is controlled by complexation with strong organic ligands (Bruland et al.,
31 1991). Copper (Cu) is probably the most studied metal in terms of organic complexation in seawater and
32 estuarine environments. This is because copper is a micronutrient, but it is also toxic, for example for
33 microalgae, at relatively low concentration levels. In addition, Cu forms complexes of relatively high
34 stability with various organic ligands. However, no many studies about copper complexation in salt-
35 marsh areas (Mucha et al., 2008) and its influence on the ligand budget of an estuary have been
36 published till these days.

37 Several sources of organic matter and ligands to estuarine and coastal areas have been pointed out in
38 the last years determining trace metal distribution along the salinity gradient (Laglera and van den Berg,
39 2003; Santos-Echeandía et al., 2008). In this way, autochthonous organisms are major producers of the
40 ligands that dominate the complexing capacity of open ocean and coastal productive waters (Croot et
41 al., 2000; Gordon et al., 2000). Organisms such as coccolithophores (Leal et al., 1999), cyanobacteria,
42 dinoflagellates (Croot et al., 2000) and heterotrophic bacteria (Gordon et al., 2000) have been observed
43 to excrete strong Cu-complexing ligands, most likely as a defense mechanism against metal toxicity. The
44 input of terrestrial humic substances through riverine waters has also been recognized as an important
45 source of strong ligands to estuarine environments (Kogut and Voelker, 2001; Shank et al., 2004a;
46 Laglera et al., 2009).

47 Recent studies have shown that estuarine sediments can also act as a significant source of Cu-
48 complexing ligands to the overlying water, which may strongly influence the biogeochemistry and
49 cycling of dissolved Cu by sediment/water exchange (Skrabal et al., 1997, 2000; Shank et al., 2004b,
50 Chapman et al., 2009). This source of organic ligands would be enhanced if sediments are colonized by
51 plants (Mucha et al., 2008). In the last years, several studies conducted in salt marsh areas, have shown
52 that as roots die they supply important quantities of organic matter to the sediment (Caçador et al.,
53 2004; Pereira et al., 2007). In addition, low molecular weight organic acids are exudated by salt-marsh

54 plant roots (Mucha et al., 2010) that can bind and redistribute metals (Mucha et al., 2008) due to their
55 high affinity to organic matter.

56 As tidal water floods the salt marsh, large quantities of organic material, nutrients and trace metals
57 accumulated in the area are exported to the estuary. On a semidiurnal tidal scale, advective fluxes are
58 enhanced in salt marsh sediments (Santos-Echeandía et al., 2010) through a mosaic of small channels in
59 the upper sediments. The relevance of the tidal induced transport on copper and complexing ligands
60 may be crucial to understand the biogeochemical cycles of metals in coastal ecosystems where salt-
61 marshes occupy large extensions.

62 Thus, the objectives of this work are: a) to measure dissolved copper and complexing ligand
63 concentrations in the Tagus estuarine waters b) to determine dissolved copper and complexing ligand
64 concentrations in the Rosário salt-marsh flooding and porewaters c) to estimate dissolved copper and
65 ligand advective fluxes in the Rosário saltmarsh d) to ascertain the importance of this input over the
66 Tagus estuarine waters.

67 **2. MATERIAL AND METHODS**

68 *2.1. Study area*

69 The 340 km² of the Tagus estuary represent one of the largest transitional systems in Europe. The
70 estuary is composed by a large shallow inner bay and a deep straight and narrow inlet channel (Fig. 1).
71 This channel reaches a depth of 40 m and constitutes the deepest part of the estuary. The bay has a
72 complex bottom topography with channels, tidal flats and islands. The deepest channel, with a water
73 depth of 5-10 m, is an extension of the inlet channel. The total amount of water in the estuary is around
74 1.9 km³. The southern and eastern parts of the bay contain extensive inter-tidal mudflats; the northern
75 part contains tidal flats, islands and several smaller channels. These channels merge upstream to a single
76 narrow channel, marking the entrance of the Tagus River.

77 The Tagus River is the main source of freshwater to the estuary. The discharge usually shows a
78 pronounced dry season/wet season as well as large inter-annual variation. The average annual discharge
79 is ~400 m³ s⁻¹, but seasonally the average monthly discharge may vary from 1 m³ s⁻¹ to > 2200 m³ s⁻¹
80 (Loureiro, 1979). Consequently, the residence time of freshwater in the estuary is highly variable and

81 may range seasonally from 6 to 65 days (Braunschweig et al., 2003). The tides are semi-diurnal, with
82 amplitudes at Lisbon ranging from ~ 1 m at neap tide to ~ 4 m at spring tide. The tidal effect reaches 80
83 km landward of the estuary mouth. Most pollutants are discharged from upper to the lower estuary (Fig.
84 1). Indeed, apart from being a major harbor, the fishing activities in the estuary are adversely affected
85 by the inflow of effluents from about 3.5 million Greater Lisbon inhabitants, part of them untreated,
86 coupled with industrial (chemicals and petrochemicals) and agricultural (fertilizers and pesticides)
87 contributions.

88 Almost 40% of the estuary is composed by inter-tidal mudflats mainly in southern and eastern shores,
89 containing extensive areas of salt marshes colonised mainly by *Sarcocornia fruticosa*, *Sarcocornia*
90 *perennis*, *Halimione portulacoides* and *Spartina maritima* occupying an area around 20 km². The marsh
91 selected for this study (Rosário) is located in the southern shoreline of the estuary (Fig.1). It covers an
92 area of 2 km² (Crespo, 1993), being characterised by homogeneous stands of *S. maritima* as a pioneer
93 species in the lower part, pure stands of *H. portulacoides* across the 20-50 cm elevation transect, and *S.*
94 *fruticosa* and *S. perennis* in the higher salt marsh. The marsh is fully inundated twice a day by tidal action
95 (2-4 m of tidal amplitude) through a highly branched system of channels that cross the elevation
96 transect. The channels have 0.5-1.5 m depth promoting the inundation of the higher marsh even at low
97 amplitude tides.

98 2.2. Sampling

99 A sampling cruise along the Tagus estuary was conducted on the 5th May 2010. A 93 m³ s⁻¹ flow was
100 measured during that day what gives a residence time around 62 days for the water in the estuary
101 (Braunschweig et al., 2003). Ten sub-surface water samples (TWB11-TWB410) were collected by hand in
102 1 L low density polyethylene (LDPE) bottles from a plastic boat (Fig. 1) during the low tide covering the
103 salinity gradient of the estuary. In addition, flooding water during tidal inundation was sampled in two
104 sites of the Rosário salt marsh (non-vegetated area and *S.maritima* colonised area and separated by less
105 than 20 m). At low tide, when sediment was exposed to the atmosphere, two sediment cores (10 cm
106 long) were collected at each site (vegetated and non-vegetated). The cores were sliced immediately
107 after sampling in two 4 cm layers, prepared composite samples for each layer of the cores collected at
108 each site, and material stored in acid pre-cleaned HDPE vials avoiding air presence inside. Sampling took

109 place in less than 3 min. Core material in the colonized area consisted of dense rooting sediments with
110 no evidence of burrowing worms, crabs or bivalves. When tidal water starts to flood each site, flooding
111 water was collected at each inundation time: 1, 5, 10, 15, 20 and 30 min for the non-vegetated area and
112 1, 5, 10, 15, 20, 30, 45 and 85 min for plant colonized area. Flooding water was sampled 1 cm above the
113 sediment surface directly into acid pre-cleaned syringes. The water and sediment samples were kept in
114 refrigerated boxes and immediately transported to the laboratory. A more detailed description of these
115 sampling procedures can be found in previous works (Caetano et al., 2007).

116 2.3. Sample treatment

117 **Estuarine and flooding water samples** were filtered through 0.45 µm cellulose membranes placed in
118 previously **acid-cleaned** filtration units (Nalgene). Filters were frozen and stored at -20°C pending
119 analysis of particulate copper and aluminium. **The main reason for measuring particulate aluminium is**
120 **that it acts as a tracer of lithogenic or terrigenous material (Windom et al., 1989; Pohl et al., 2004) and**
121 **will be useful for the interpretation of the various sources of material to estuarine waters (i.e. rivers or**
122 **sediment resuspension) (Mota et al., 2005).**

123 Pore waters were separated from the sediment layers by centrifugation at 10,160 rcf_{xg} for 30 min at +4
124 °C and filtered through 0.45 µm cellulose acetate membranes. Filtration and subsequent manipulation
125 of the samples were carried out in a glove box under argon atmosphere in order to avoid alteration of
126 the initial conditions (Caetano et al., 2007; Santos-Echeandia et al., 2009). A portion of the filtered
127 samples (around 200 mL) was frozen for speciation analysis while around 100 mL were acidified with
128 suprapure HCl (pH < 2) and stored pending analysis of total dissolved copper.

129 2.4. Copper analysis in *estuarine water*

130 2.4.1. Total dissolved copper concentrations

131 Copper analyses were carried out using voltammetric equipment (Metrohm 797 VA Computrace)
132 controlled by a computer (PC). The reference electrode was a double junction, Ag/AgCl, KCl (3 M),
133 saturated AgCl, with a salt-bridge filled with 3 M KCl, and the counter electrode was a glassy carbon rod.
134 A hanging mercury drop electrode (HMDE) was used as the working electrode. The copper
135 concentration in the filtered samples was determined using a procedure similar to the one described

136 previously (Campos and van den Berg, 1994). **Estuarine and flooding water** was UV-digested (1 h) after
137 acidification to pH 2.2 by the addition of 10 μ L 6 M bidistilled HCl (AnalR BDH) per 10 mL of sample in
138 acid-cleaned borosilicate glass tubes. A 10 mL sample aliquot was pipetted into the voltammetric cell
139 and ammonia (AristarGrade Merck) was used to ascertain the approximate neutralization of the pH;
140 also, HEPES buffer (BDH, final concentration 0.01 M) and Salycildoxime (SA, Sigma, final concentration of
141 25 μ M SA) were added. The solution was deaerated by purging (5 min) with nitrogen. The voltammetric
142 parameters were: deposition 60 s at -1.1 V whilst stirring, 8 s quiescence at -0.1 V, and a potential scan
143 using the square-wave modulation: 10 Hz, step height 2.5 mV, pulse height 25 mV, from 0 to -0.8 V. The
144 sensitivity was calibrated by incorporating standard copper additions (Spectrosol BDH) to each sample.
145 **Each sample was analyzed in triplicate.** A blank with Milli-Q water (18.2 M Ω .cm) was made at intervals
146 of every three samples and its concentration was subtracted in order to eliminate any copper
147 contribution from reagents. Blank concentrations were around 0.27 \pm 0.06 nM.

148

149 *2.4.2. Copper titrations*

150 The copper complexing capacity of the waters of the Tagus estuary was determined by competing ligand
151 exchange with adsorptive cathodic stripping voltammetry (CLE-AdCSV) of Cu-salycilaldoxime (SA)
152 complexes according to previous works on copper complexation in estuarine waters (Campos and van
153 den Berg, 1994; Laglera and Van Den Berg, 2003). Briefly, a 170-ml sample previously filtered by **0.45 μ m**
154 was transferred to a polyethylene bottle (Nalgene), and spiked with HEPES/NH₄OH buffer (for a
155 concentration of 0.01 M) and SA (mix concentration of 5 or 10 μ M). After stirring, 10 mL aliquots were
156 pipetted into **15 polystyrene vials (30 mL Bibby, Sterilin)** that were previously spiked with copper to
157 provide increasing concentrations in the range of 0–700 nM (actual range depending on the initial
158 copper concentration and the ligand concentration to be determined). **Prior to the first titration, the**
159 **tubes were conditioned twice overnight with seawater containing the same range of copper**
160 **concentrations in order to avoid copper loss in the tube walls. After that, aliquots of each sample were**
161 **left to equilibrate overnight at room temperature due to the slow kinetics of the ligands and copper**
162 **reactions (Campos and van den Berg, 1994).** The equilibrium concentration of Cu-SA complexes was
163 determined using the following parameters: adsorption potential of -0.15 V, deposition time of 60 s, 8 s

164 quiescence, potential scan from 0 to -0.8 V using square-wave modulation at 10 Hz, step height 2.5mV
165 and pulse height of 25 mV.

166 2.4.3. Evaluation of complexing capacities and conditional stability constants

167 Changes in the ratio between the concentrations of CuSA (labile to AdCSV) and CuL in the different
168 aliquots permit the determination of the copper complexing capacity of the ligands present in solution
169 (C_L) and their conditional stability constant to bind copper (K'_{CuL}). A more detailed explanation can be
170 found elsewhere (Ruzic, 1982; van den Berg, 1982). The relationship between the different copper
171 fractions is described by the following transformation of the Langmuir isotherm:

$$172 \quad [Cu]_{TOT} = \sum (C_{Li} [Cu]_{lab} / K'_{CuLi\alpha'} + [Cu]_{lab}) + [Cu]_{lab} \quad (1)$$

173 L_i represents the variability of the nature of the different natural ligands. Those ligands are
174 differentiated according to the stability of their complexes with copper. α' is the α -coefficient of Cu^{2+}
175 with inorganic ligands and SA. $[Cu]_{TOT}$ and $[Cu]_{lab}$ are respectively the total and labile copper
176 concentrations related by:

$$177 \quad [Cu]_{TOT} = \sum [CuLi] + [Cu]_{lab} = \sum [CuLi] + [Cu(SA)] + [Cu(SA)_2] \quad (2)$$

178 The concentration of labile copper is calculated from:

$$179 \quad [Cu]_{lab} = i_p / S \quad (3)$$

180 Where i_p is the voltammetric signal obtained from the reduction of the CuSA complexes adsorbed on the
181 HMDE electrode and S is the ratio signal/concentration or sensitivity. S can be estimated from the slope
182 of the last few points of the titration (S^{INT}) if the titration has been extended to copper concentrations
183 enough to complete the saturation of the natural ligands.

184 As indicated in the previous section, samples were analyzed using two different SA concentrations (5
185 and 10 μ M). Higher SA concentrations increase the competing ability of SA. In the presence of complex
186 mixes of ligands characterized by the formation of complexes with copper in a wide range of stability
187 constants, the effect of increasing the SA concentration is both, an overcompetition of those ligands of
188 low affinity for copper and the equilibration of SA with ligands of very high stability constant. Therefore,
189 in heterogeneous matrices, the shift of the SA concentration resolves a different fraction of ligands,

190 fraction that is defined as detection window. This is an important tool to estimate the heterogeneity of
191 the pool of copper ligands in the sample.

192 Values for the stability constants of the complexes CuSA and Cu(SA)_2 are necessary in order to obtain
193 the value of α' at each salinity. Both stability constant were calculated using relationships obtained in a
194 previous work (Campos and van den Berg, 1994):

$$195 \quad \log K_{\text{CuSA}} = (10.12 \pm 0.03) - (0.37 \pm 0.02) \log \text{salinity} \quad (4)$$

$$196 \quad \log \beta'_{\text{Cu(SA)}_2} = (15.78 \pm 0.08) - (0.53 \pm 0.07) \log \text{salinity}. \quad (5)$$

197 A plot of $[\text{Cu}]_{\text{lab}}$ vs the ratio $[\text{Cu}]_{\text{lab}}/[\text{CuL}]$ is the most used procedure to solve C_L and K'_{CuL} from the slope
198 and the Y-axis value respectively. When only one ligand is present, the data follow a straight line but if
199 more than one type of ligands are present, the plot takes a curved shape. In this case C_L and K'_{CuL} can be
200 calculated with accuracy for a maximum of two types of ligands.

201 The estimation of C_{L1} , K'_{CuL1} , C_{L2} and K'_{CuL2} requires either an iterative refine procedure (Laglera-Baquer et
202 al., 2001; van den Berg, 1982) or a nonlinear fitting (Gerringa et al., 1995). In the first case the solutions
203 for C_{L1} and K'_{CuL1} are refined with estimations of C_{L2} and K'_{CuL2} from different linear sections of the plot
204 until a convergent solution is obtained.

205 Complexing capacities, conditional stability constants and S can also be obtained fitting non-linearly the
206 substitution of Eq(3) in Eq(1). Non-linear fitting prevents the uncertainty caused by the arbitrary
207 necessity to split the titration data in two that iterative linear fitting requires.

208 In this work, we have used the fitting tool of a popular computer program, SigmaPlot (© Systat
209 Software, Inc) to fit 3, 4 or 5 parameters. The program uses a Levenberg-Marquardt fitting algorithm.
210 We first solved the titration data sets for the hypothesis of a single ligand model using non-linear fitting
211 incorporating S as a parameter to C_L and K. For this purpose, a new equation was incorporated to the
212 Regression Wizard of the software under the "User-Defined" category. The Code fed to the Regression
213 Wizard is presented in Table S1.

214 Then, we prepared a new Equation for the case of two types of ligands, i.e. 5 parameters (C_{L1} , K'_{CuL1} , C_{L2}
215 and K'_{CuL2} and S) but the program struggled to offer realistic values in the form of very high S and K'_{CuL1}
216 values. Removal of S from the list of parameters and use of S^{INT} did not solve problems with K'_{CuL1} for

217 some titrations. In those cases, K'_{CuL1} was obtained from the iterative linear routine and its value fixed in
218 the *constrains* section of the code (Table S1) during the non-linear fitting of the rest of the complexing
219 parameters.

220 2.4.4. Particulate copper and aluminum

221 In order to determine the amount of labile copper, filters obtained from filtered water were subject to
222 digestion overnight with 0.1 M acetic acid in Teflon® vials (Savillex) at ambient temperature following
223 the first step of the BCR extraction procedure (European Community Bureau of Reference; Quevauviller
224 et al., 1997). The digest was then syringed-filtered (0.45 µm) using a Swinnex filtration unit and stored
225 pending analysis; filters containing the remnant particles were microwave digested using a mixture of
226 HF and HNO₃ (1:3) in order to analyze the total fraction (Biscombe, 2004).

227 Labile copper determination was carried out by means of cathodic stripping voltammetry as explained
228 before (Campos and van den Berg, 1994) while total particulate copper and aluminum determination
229 was carried out with the standard additions method. Concentrations of Al and Cu were determined
230 using a quadrupole ICP-MS (Thermo Elemental, X-Series) equipped with a Peltier Impact bead spray
231 chamber and a concentric Meinhard nebulizer. Coefficients of variation for metal counts ($n = 5$) varied
232 between 0.5 and 2%. The precision and accuracy of each metal concentration measurements,
233 determined through repeated analysis of certified reference material (PACS2), using Indium as internal
234 standard, were 1–4% and 2–5%, respectively (data not shown). Procedural blanks always accounted for
235 less than 1% of the total metal concentrations in samples.

236 2.5. Estimation of sediment-water interchange: tidal induced fluxes

237 As water floods over inter-tidal sediments the pore water solutes tend to be exported by advection
238 and/or exchanged between mixing top sediments and tidal water. The associated pressure difference
239 and tidal water movement are the driven mechanism for this transport. By using the temporal variation
240 of copper and ligand concentrations in the flooding water the tidal induce transport (T) to the water
241 column is calculated using the following expression (Caetano et al., 2007).

$$242 \quad T = \sum [(C_{t+1} - C_t)/(2 - C_i)](h_{t+1} - h_t) \quad (6)$$

243 where C_{t+1} and C_t are solute (copper and ligand) concentrations in the flooding water at times $t+1$ and t ,
244 C_i is the residual concentration (lowest value obtained for the flooding water) and h_t and h_{t+1} are the
245 water depth at the same times. It was observed that water depth during the field measurements
246 increased on the average 0.5 and 0.8 cm per minute of inundation in *S. maritima* and non-vegetated
247 areas, respectively. The tidal induced transport of trace metals is calculated for the first 85 and 30 min
248 of inundation, respectively. Since inter-tidal sediments are inundated twice a day, the tidal induce
249 transport (T) was multiplied by a factor of two to present values on a daily basis.

250 *2.5. Statistics*

251 *The statistical analyses were performed using STATISTICA 6 (Statsoft).*

252 **3. RESULTS**

253 *3.1. Determination of the complexing parameters and the sensitivity by non-linear fitting*

254 Table 1 shows the complexing parameters found for the estuarine **water** samples according to one and
255 two ligands models. Table 2 shows those parameters for flooding waters and interstitial waters
256 extracted from cores. For the one ligand model, S was added to the fitting procedure according to the
257 code shown in Table S1. Values for S were in the range 94-113 % with respect to S^{INT} (average 98.9 ± 4.1
258 %) indicating that any bias due to undersaturation of the ligands present in the sample caused by a too
259 small copper concentration at the end of the titration was masked by the analytical error. For the
260 sample collected at station 11, S was fitted at a very low value 90% of S^{INT} and the complexing
261 parameters were recalculated using S^{INT} .

262 For the two ligands model, this approach was not possible as explained above. For some titration sets, S
263 was estimated to be 103-114 % of S^{INT} but for many others this correction reached as much as 170 %
264 which could be discarded simply by visual inspection. Values in Table 2 were obtained using S^{INT} . When
265 the estimation of K'_{CuL1} produced a value over 20, the titration data set was solved by iterative linear
266 fitting (Laglera-Baquer et al., 2001; Laglera and Van Den Berg, 2003) and the value of K'_{CuL1} fixed on the
267 constrains section of the code. **This** led to a 3 parameters non-linear fitting. An extensive description of
268 the routine to fit complexing parameters out of metal titration data sets used here is presented in a
269 separate work (Laglera et al., 2012).

270 3.2. Dissolved copper and its organic speciation in the Tagus estuary

271 Dissolved copper concentrations along the salinity gradient in the Tagus estuary are plotted in Fig. 2a.
272 With the exception of the station located upstream in the river (26.4 nM), values were quite constants
273 and around 20 nM all over the estuary. The ligand concentration (L; Fig. 2a), for the 5 μ M SA detection
274 window, showed higher values in riverine samples (399 nM) decreasing to 320-340 nM in the first 3
275 units of salinity. A new decay is found from salinity 5 to 25 (to 46 nM). This decreasing trend from fresh
276 to marine waters has been observed before in other estuarine systems (Laglera et al., 2003; Plavsic et
277 al., 2009). The conditional stability constant for these ligands ($\log K'$) ranges between 12.20 and 13.26
278 (Table 1), and it presents a bowl-shape distribution along the salinity gradient, with lower values in the
279 mid-estuary and maxima at marine (13.26) and riverine (13.11) end-members.

280 By fitting data to two types of ligands, a strong (L_1) and a weak (L_2) one can be observed in the Tagus
281 estuary waters (Fig. 2a). Ligand L_1 varied between 14 and 55 nM being the highest concentration found
282 in the two most riverine stations. Values decreased sharply to 15 nM at salinity 3 remaining almost
283 constant until the marine end member (salinity 25). Otherwise, L_2 concentrations vary between 36 and
284 368 nM with a conservative distribution between salinities 5 and 25, but with lower values than
285 expected for an ideal dilution line between salinities 0 and 5. The conditional stability constants for
286 these ligands range between 14.10 and 15.75 for L_1 and between 12.06 and 13.13 for L_2 (Table1). The
287 distribution along the salinity gradient is different among them; while $\log K_1'$ shows a saw tooth
288 tendency with higher values in the riverine end-member, $\log K_2'$ distribution is comparable to $\log K'$,
289 with the lowest values in the mid estuary and increasing towards the river (13.13) or the sea (12.42) end
290 members.

291 In order to detect stronger copper complexing ligands and check for homogeneity/heterogeneity of
292 them in the estuary (van den Berg and Donat, 1992; Buck and Bruland., 2005; Santos-Echeandia et al.,
293 2008), a detection window of 10 μ M SA has been applied to some of the samples. Samples, fitted to one
294 ligand are plotted in Fig. 2b. Ligand concentration increases between salinity 0 and 5 (from 121 to 142
295 nM) and progressively decreases to 30 nM at salinity 25 with a quite linear trend. The conditional
296 stability constant ($\log K'$) presented, again, lower values at mid salinities (13.11) increasing towards the
297 riverine (14.52) and marine (13.76-14.15) end members (Table 1) as observed for the lower detection

298 window (5 μM SA). By fitting data to two types of ligands, the strongest one (L_1) concentrations ranged
299 between 15 and 28 nM (Fig. 2b) with a quite irregular distribution. On the contrary, the weakest ligand
300 of this detection window (L_2) shows a similar trend to L_1 , with an initial increase from 145 to 174 nM
301 decreasing progressively afterwards to 22 nM at salinity 25. The conditional stability constants, both \log
302 K_1' and $\log K_2'$ present higher values at low salinities (16.84 for K_1 and 13.87 for K_2) that sharply
303 decreased at salinity 5 reaching 15.02 for $\log K_1'$ and 12.76 for $\log K_2'$ remaining relatively constant
304 towards the marine end-member (Table 1).

305 *3.3. Suspended Particulate Matter, particulate total and labile copper and aluminium concentrations in* 306 *the Tagus estuary*

307 Suspended particulate matter values oscillate between 4.8-14.7 mg L^{-1} in the estuary with an irregular
308 distribution (Fig. S1a). The highest values were found at salinities 10-15 and the lowest between
309 salinities 19-23. Particulate copper concentrations varied between 0.78 and 14.8 nM (Fig. S1b). The
310 highest levels were found at mid-salinities (5-15 ups) while the lowest values measured at both end-
311 members. The labile copper in the particulate matter accounts only for the 0.05-0.45 % of the total
312 copper but it is noticeable that the lability was higher for the lowest salinities (Fig. S1c). Particulate
313 aluminum concentrations ranged between 272 and 4930 nM with a similar distribution to particulate
314 copper.

315 *3.4. Dissolved copper and its organic speciation in the Rosario Saltmarsh*

316 *3.4.1. Flooding waters*

317 Dissolved copper concentrations in the flooding water in the two sites of the salt marsh (non-vegetated
318 and plant colonized areas) are plotted in Fig. 3a. Copper levels in the non-vegetated zone increase 1
319 minute after arriving of tide water from 18.3 to 28.5 nM. In the following 5 minutes, levels decreased
320 reaching 20.6 nM and remaining quite constant until 30 minutes after tidal inundation started, with the
321 exception of minute 15 when a less pronounced increase (27.0 nM) was observed (Fig. 3a). In a similar
322 way, dissolved copper levels increased in the colonized area 1 minute after the flood started reaching
323 higher values (32.5 nM) than in the non-vegetated area. Afterwards, concentrations decreased to 17.7
324 nM and varied irregularly between 13.6 and 22.1 nM during the next 80 minutes of inundation.

325 The time course evolution of ligand concentration in the flooding waters is also plotted in Fig. 3a. A net
326 increase of its concentration (initial levels of 46 nM) was observed in both sampling areas but reaching
327 higher concentrations in the plant colonized (291 nM) than in the non-vegetated area (85 nM) during
328 the first minute of inundation. Afterwards levels in plant colonized sediments decreased sharply while in
329 non-vegetated area values diminished progressively reaching, at both areas similar values to those
330 found before inundation started. The conditional stability constants of ligand showed higher values in
331 the non-vegetated (13.73-14.04) than in the plant colonized area (13.11-13.89) (Table 2). The
332 significance for statistical analyses was $p < 0.05$.

333 In addition, the time course evolution of $\log K'$ values during the tidal inundation were different among
334 the two sites: while an increase of $\log K'$ was found one minute after the inundation started in the non-
335 vegetated area, a progressive increase of $\log K'$ with time was observed in the vegetated area during the
336 first 10 minutes.

337 The strongest ligand (L_1) concentrations vary between 46 and 61 nM in the non-vegetated area without
338 a trend all over the time (Fig. 3b). Nevertheless, L_1 concentrations in the colonized area are more
339 variable and ranged between 28 and 95 nM. The conditional stability constant of this ligand varied
340 between 14.12 and 14.79 in the non-vegetated area while in the colonized area a variation between
341 13.61 and 14.83 was found (Table 2). The weakest ligand concentrations were higher and varied
342 between 60 and 107 nM for the non-vegetated area and from 5.5 to 258 nM for the colonized area (Fig.
343 3b). It is noticeable the net increase in the colonized area in the first minutes of inundation that is not
344 observed in the non-vegetated area. Finally, conditionals stability constant for this weakest ligand
345 oscillate between 11.95-12.26 nM in the non-vegetated area and 11.87-13.05 in the colonized area
346 (Table 2).

347 Strongest ligands have been detected in the flooding waters moving the detection window to 10 μ M SA.
348 Ligand concentration were lower (61-87 nM) in the non-vegetated area than in the colonized site (107-
349 137 nM) during the first 5 minutes of inundation (Fig. 3c). An increase was found in the first minute
350 comparing to the estuarine waters in the vicinity of the salt-marsh and concentrations slightly decrease
351 after 5 minutes. The respective conditional stability constants were similar in the non-vegetated area
352 (14.39-14.48 nM) and in the plant-colonized area (14.32-14.47 nM) (Table 2).

353 Two types of strong ligands were found in the colonized area with concentrations ranging between 58
354 and 82 nM for L_1 and from 59 to 138 nM for L_2 with a similar trend to the unique ligand (L). However, L_1
355 levels do not decrease after 5 minutes but continue to increase (Fig. 3c). Conditional stability constants
356 ranged in the following intervals: 14.63-15.69 for L_1 ; and 12.84-13.44 for L_2 (Table 2).

357 3.4.2. Porewaters.

358 Dissolved copper and ligand concentrations and their conditional stability constants in the porewaters of
359 the salt-marsh are shown in Table 3. Levels of dissolved copper in the non-vegetated area ranged from
360 45.3 to 53.9 nM with higher values in the upper layer than in the deeper one. However, higher ligand
361 concentrations were found in deeper porewaters (321 nM) than in surface ones (245 nM). The
362 conditional stability constants for these ligands varied between 13.24 for the deeper layer and 13.58 for
363 the upper one. Levels of the stronger ligand (L_1) ranged from 77 to 184 nM with higher values in the
364 upper layer. Nevertheless, the conditional stability constant was higher (14.77) in the deeper layer than
365 in the upper one (13.70). Concentrations of L_2 varied between 70 and 287 nM with increased values in
366 the deeper layer. The conditional stability constants of this weakest ligand were 12.68 for the deeper
367 layer and 13.09 for the upper one.

368 Higher dissolved copper concentrations in pore waters (71-142 nM) were found in the plant colonized
369 area (Table 3). Ligand concentrations vary between 767 nM in the deeper layer and 831 nM in the upper
370 one. Conditional stability constant for this ligand showed higher values in the upper layer. The stronger
371 ligand, L_1 , levels varied between 115 and 203 nM with higher values in the upper layer and their
372 conditional stability constants were 15.17 for the upper layer and 14.66 for the deeper one.
373 Concentrations of L_2 were quite similar among layers (666 and 699 nM) as the conditional stability
374 constants (13.09 and 12.82).

375 Strongest ligands in pore waters were found by applying a higher detection window (10 μ M) (Table 3).
376 Ligand concentration in the non-colonized area was 230 nM with a conditional stability constant of
377 14.28. A strong ligand with a $\log K_1'$ of 15.25 and a concentration of 67 nM and a weak ligand with a \log
378 K_2' of 13.85 and a concentration of 182 nM result from the data fitting to two types of ligands. As found
379 with the 5 μ M SA detection window, higher values were observed in the vegetated area at 10 μ M
380 detection window. A ligand concentration of 419 nM with a $\log K'$ of 13.95 was registered. In the data

381 fitting to two types of ligands, a strong ligand concentration of 148 nM with a log K_1' of 17.56 was
382 recorded, while the weakest ligand showed a concentration of 846 with a log K_2' of 13.51.

383 *3.5. Tidal induced transport of copper and organic ligands in the Rosario Saltmarsh*

384 An estimation of the tidal induced transport of dissolved copper and ligands is shown in Table 4. A flux
385 of $1.23 \mu\text{mol m}^{-2} \text{d}^{-1}$ of dissolved copper escapes from the sediment to the overlying waters in the non-
386 vegetated area, while the ligand transport was $3.25 \mu\text{mol m}^{-2} \text{d}^{-1}$. If the two ligand case is considered, an
387 export of $2.16 \mu\text{mol m}^{-2} \text{d}^{-1}$ of the strongest ligand and $2.31 \mu\text{mol m}^{-2} \text{d}^{-1}$ of the weakest one was
388 estimated. As expected from the results shown in previous sections calculated transports are higher in
389 the plant colonized area, where a $2.43 \mu\text{mol m}^{-2} \text{d}^{-1}$ flux of dissolved copper is estimated. The ligand flux
390 ($48.2 \mu\text{mol m}^{-2} \text{d}^{-1}$) was around fifteen times higher than in the non-vegetated area. Increased transport
391 of both strong and weak ligand to the water column was also found with $11.5 \mu\text{mol m}^{-2} \text{d}^{-1}$ for L_1 and
392 $64.7 \mu\text{mol m}^{-2} \text{d}^{-1}$ for L_2 .

393 The tidal induced transport of ligands detected by the $10 \mu\text{M}$ SA detection window was similar in the
394 non-vegetated area and lower in the colonized area. In this way, $4.25 \mu\text{mol m}^{-2} \text{d}^{-1}$ of ligands were
395 exported in the non-colonized area while $6.87 \mu\text{mol m}^{-2} \text{d}^{-1}$ were exported in the plant colonized area.
396 For the two ligand case, $3.80 \mu\text{mol m}^{-2} \text{d}^{-1}$ of the strongest ligand and $5.77 \mu\text{mol m}^{-2} \text{d}^{-1}$ of the weakest
397 one were estimated.

398 **4. DISCUSSION**

399 *4.1. Copper and organic ligands behavior during the estuarine mixing*

400 Dissolved copper and complexing ligand behavior in the Tagus estuary can be clearly divided in two
401 distinct chemical areas. The edge is marked by the salinity 5.6 sample. In the low salinity stretch,
402 although dissolved copper values were only higher in the most riverine sample, the strong ligand values
403 (L_1) were higher than in the rest of the estuary. As a consequence the L_1/Cu ratio is relatively constant
404 and around 1. The only exceptions are the two most riverine stations (Fig. S2) where an excess of L_1 ,
405 which may derived from the river end member was detected. This ratio is linear and progressively
406 decreases with the increasing salinity if total ligand concentration is considered (Fig. S2). Moreover, the
407 weakest ligand (L_2) also showed a different behavior in this zone of the estuary but with lower levels

408 than expected if the trend marked by the seven most saline stations is extended to the freshwater end-
409 member.

410 The mixing of freshwater with the marine water dilutes L_1 ligand within the estuarine area. The long
411 residence times (Braunschweig et al., 2003), confirmed by uniform suspended particulate matter
412 content in a wide salinity range (Fig. S1a), allow the homogenization of the water body justifying the
413 constancy of copper and strong ligand levels in the 6-25 salinity range. This pattern suggest that the tidal
414 effect superimposes the river flow and no losses of copper or strong ligands occurred during the
415 estuarine mixing. Similar findings have been observed in the Scheldt estuary by Laglera and van den
416 Berg (2003). A continuous lateral input, as detected in the Vigo Ria (Santos-Echeandía et al., 2008), in
417 the Tagus estuary may also explain the constant values all over the salinity gradient. In addition, this
418 area shows constant and close to the unit L_1/Cu ratios in a wide salinity range (Fig. S2). This means that
419 copper and L_1 levels are similar probably because their source is the same. There is no evidence of
420 copper transfer from the dissolved to the particulate fraction since values were quite low all through the
421 estuary (Fig. S1b). However, L_2 experiments a progressive decrease in their levels towards the outer part
422 of the estuary and no remarkable inputs of L_2 are observed at mid-high salinities as observed for L_1 . It
423 can be assumed that the river is not the major source of this weak ligand, but its origin is somewhere in
424 between salinities 0-6, where although the mixing with seawater, its concentration remains constant or
425 even increases. This increase is consistent with the trend observed at both detection windows for the
426 weakest ligand (Fig. 2). The higher particulate aluminum concentrations at salinities 6-10 (Fig. S1c) and
427 SPM at salinity 10 could reflect the maximum turbidity zone in this salinity gradient and at spring tides
428 the bottom particle resuspension in this area may explain the release of the weakest ligand from the
429 sediments (Shank et al., 2004; Santos-Echeandia et al., 2008). If copper variability during the estuarine
430 mixing is associated to L_1 , L behavior is ruled by L_2 . This fact is supported by the spatial distribution of log
431 K'_2 , which is quite similar to log K' (Table 1) at both detection windows (5 μM y 10 μM).

432 Regarding the nature of the ligands, by comparing L_1 with L_2 at both detection windows, the distribution
433 of the stronger ligand (L_1) was homogeneous, mainly at high salinities, because the log $K'_{1,5\mu MSA}$ and log
434 $K'_{1,10\mu MSA}$ were similar (Table 1) and, in general, their ratio was close to 1 (Fig.S3a). Moreover, ratios
435 between L_1 measured at the low detection window and the L_1 observed at the high detection window

436 were closer to 1 (1.24 ± 0.33) along the salinity gradient (Fig.S3b). Conversely, L_2 was very heterogeneous
437 and a shift to the higher detection window induces the decrease of the ligand concentrations. Thus, the
438 ratio between L_2 measured at low detection window and at high detection window is around 2
439 (2.09 ± 0.48) (Fig. S3b). An increase of the log K' values is also observed when moving the detection
440 window to 10 μM SA. As a consequence the ratios between log K' at high and low detection windows are
441 always well below 1 all over the salinity gradient (Fig. S3a).

442 *4.2. Saltmarsh inputs of copper and complexing ligands to the estuary*

443 Intertidal and saltmarsh areas constitute one of the possible sources of copper and complexing ligands
444 to estuarine waters. Mucha et al. (2008) demonstrated that salt-marsh plants are able to produce
445 relatively high amounts of strong Cu-complexing ligands in their root system and the present study
446 evidenced that these complexes are exported to estuarine waters through tidal induced transport (Table
447 4).

448 The constant dissolved copper and L_1 concentrations in a wide salinity gradient (6-25) is presumably
449 explained by the lateral input from the marsh areas along the gradient coupled with high residence time
450 of water in the estuary. Previous studies have showed that copper levels in the adjacent area to the
451 Tagus ($S \geq 30$) varied between 1.6 and 14.6, well below the values found at salinity 25 (Cotté-Krieff et al.,
452 2000; Santos-Echeandia et al., 2012). The correlation between Cu and L_1 ($r=0.67$, $p<0.05$) in the Tagus
453 estuarine waters suggest that the source of copper and ligands at mid-salinities is diluted at high
454 salinities. The inexistence of marshes downstream the inlet that connects the estuary to the sea
455 reinforces the hypothesis that salt marshes are the main source of copper and complexing ligands.
456 Moreover, the conditional stability constants for L_1 in the waters exported from the salt-marsh
457 (14.34 ± 0.27 for the non-colonized area and 14.17 ± 0.41 for the vegetated area) are comparable to the
458 ones present in the estuary (14.38 ± 0.37).

459 Although the conditional stability constants for L_2 in the waters derived from salt-marshes (12.12 ± 0.14
460 for the non-colonized area and 12.29 ± 0.46 for the vegetated area) are similar to those present in the
461 estuary, the input through tidal cycles is not reflected in the estuarine distribution of the weak ligand. As
462 shown before, L_2 concentrations decrease towards higher salinities. A photo-degradation process during
463 the transportation of these ligands to estuarine water with low particulate matter concentrations (5-15

464 mg L⁻¹ against 22-99 mg L⁻¹ for the Scheldt estuary, Zwolsman and van Eck., 1999) is a possible
465 explanation. The high residence time of the waters in the Tagus estuary would favor this degradation as
466 shown in the Scheldt estuary (Laglera and van den Berg., 2006). According to these authors L₂ is more
467 susceptible to photo-degradation than L₁, as the former is stabilized by its complexation with copper. In
468 addition, due to the heterogeneous distribution of this ligand, it is possible that several sources (i.e.
469 harbor, untreated effluents) contribute to the pool of weak ligands.

470 Considering the water volume of the Tagus estuary (1.9x10⁹ m³), the residence time during the sampling
471 conditions (60 days), the area covered by the intertidal non-vegetated zones (128 km²) and salt marshes
472 (20 km²) and the tidal induce transport of copper and ligands from the sediment to the water column in
473 the Rosário salt-marsh (Table 4), a contribution of around 7 nM of copper, 16 nM of L₁ and 52 nM of L₂
474 to the Tagus estuarine waters has been estimated. This account for 35% of Cu, 94% of L₁ and 45% of L₂
475 present in the estuary (S≥6).

476 This continuous input of copper complexing ligands is beneficial for the health of the estuary. Several
477 inputs of copper coming from a variety of sources, especially in such an industrialized and populated
478 area as it is the Tagus estuary can be neutralized by its binding to natural ligands. This would decrease
479 its toxicity to living organisms when an extra input of copper occurs (Louis et al., 2009).

480 5. CONCLUSIONS

481 Tagus estuarine waters show a relatively constant copper concentration during the estuarine mixing.
482 Most of this copper is organically complexed by a strong ligand (L₁) all through the estuary. A second and
483 weakest ligand (L₂) was also detected in these waters in higher concentrations. Salt-marsh areas are the
484 major sources of copper complexing ligands to the Tagus estuary. Noticeable, tidal induced transport
485 continuously feed estuarine waters with copper and ligands, mainly with the strongest one. Its input can
486 represent 95% of the ligand present in the estuary. Salt-marsh input of copper complexing ligands
487 determines copper distribution along the salinity gradient of the Tagus estuary.

488 Although future research should be performed to compare the importance of this source of ligands with
489 other sources like urban effluents, rivers or benthic inputs, the present work has demonstrated that salt
490 marsh areas are the main inputs of copper complexing ligands to the Tagus estuary.

491 This type of fluxes should be taken into account when assessing trace metal contamination problems
492 and remediation in estuarine and coastal areas. Furthermore, one may speculate that inundation of
493 coastal areas associated with the climatic changes, either to increase of water levels or floods will result
494 in additional fluxes of trace elements and copper complexing ligands from inter-tidal areas to estuarine
495 and coastal waters. The relevance of the tidal induced transport on copper and complexing ligands
496 coming from salt marsh areas may be crucial to understand the biogeochemical cycles of metals in
497 coastal ecosystems all over the world where salt-marshes occupy large extensions.

498

499 **Acknowledgements.** The authors would like to thank Vasco, Rute and Antonio for their kind sampling
500 cooperation during the sampling campaign. The C.S.I.C., under the program JAE-Doc (*Junta para la*
501 *Ampliación de Estudios*) co-funded by the *European Social Fund* (ESF), is greatly acknowledged for the
502 post-doctoral contract to J. Santos-Echeandía.

503 REFERENCES

- 504 - Biscombe., 2004. Factors influencing the seawater solubility of aerosol associated trace metals. PhD
505 Thesis. University of Plymouth.
- 506 - Braunschweig, F., Martins, F., Chambel, P., Neves, R., 2003. A methodology to estimate renewal time
507 scales in estuaries: the Tagus Estuary case. *Ocean Dynamics* 53, 137-145.
- 508 - Bruland, K.W., Donat, J.R., Hutchins, D.A., 1991. Interactive influences of bioactive trace metals on
509 biological production in oceanic waters. *Limnology and Oceanography* 36, 1555-1577.
- 510 - Buck, K., Bruland, K., 2005. Copper speciation in San Francisco Bay: a novel approach using multiple
511 analytical windows. *Marine Chemistry* 96, 185-198.
- 512 - Caçador, I., Costa, A., Vale, C., 2004. Carbon Storage in Tagus Salt Marsh Sediments. *Water Air Soil*
513 *Pollution: Focus* 4, 701-714.
- 514 - Caçador, I., Vale, C., Catarino, F., 1993. In: Vernet, J.-P. (Ed.), *Environmental contamination. Studies in*
515 *Environmental Science* vol. 55. Elsevier, Amsterdam, pp. 355-365.

- 516 - Caetano, M., Fonseca, N., Cesário, R., Vale, C., 2007. Mobility of Pb in salt marshes recorded by total
517 content and stable isotopic signature *Science of the Total Environment* 380, 84-92.
- 518 - Campos, M.L.A.M. and van den Berg, C.M.G., 1994. Determination of copper complexation in sea
519 water by cathodic stripping voltammetry and ligand competition with salicylaldoxime *Analytica*
520 *Chimica Acta* 284, 481-496.
- 521 - Chapman, C.S., Capodaglio, G., Turetta, C., van den Berg, C.M.G., 2009. Benthic fluxes of copper,
522 complexing ligands and thiol compounds in shallow lagoon waters. *Marine Environmental*
523 *Research* 67, 17-24.
- 524 - Cotté-Krieff, M.H., Guieu, C., Thomas, A.J., Martin, J.M., 2000. Sources of Cd, Cu, Ni and Zn in
525 Portuguese coastal waters. *Marine Chemistry* 71 (3-4), 199-214.
- 526 - Crespo, R., 1993. Cartografia do habitat potencial de passeriformes no Estuário do Tejo por
527 processamento digital de imagem. Degree Thesis. Faculdade de Ciências — Universidade de
528 Lisboa, Portugal, pp. 124.
- 529 - Croot, P.L., Moffet, J.W., Brand, L.E., 2000. Production of extracellular Cu complexing ligands by
530 eucaryotic phytoplankton in response to Cu stress. *Limnology and Oceanography* 45, 619-627.
- 531 - Gerringa, L.J., Herman, P.M., Poortvliet, T.C., 1995. Comparison of the linear Van den Berg/Ruzic
532 transformation and a non-linear fit of the Langmuir isotherm applied to Cu speciation data in the
533 estuarine environment. *Marine Chemistry* 48, 131-142.
- 534 - Gordon, A.S., Donat, J.R., Kango, R.A., Dyer, B.J., Stuart, L.M., 2000. Dissolved copper-complexing
535 ligands in cultures of marine bacteria and estuarine water. *Marine Chemistry* 70, 149-160.
- 536 - Kogut, M.B., Voelker, B.M., 2001. Strong copper-binding behavior of terrestrial humic substances in
537 seawater. *Environmental Science and Technology* 35, 1149-1156.
- 538 - Laglera-Baquer, L.M., González-Dávila, M., Santana-Casiano, J.M., 2001. Determination of metallic
539 complexing capacities of the dissolved organic material in seawater. *Scientia Marina* 65, 33-40.

- 540 - Laglera, L.M., van den Berg, C.M.G., 2003. Copper complexation by thiol compounds in estuarine
541 waters. *Marine Chemistry* 82 (1–2), 71–89.
- 542 - Laglera, L.M., van den Berg, C.M.G., 2006. Photochemical oxidation of thiols and copper complexing
543 ligands in estuarine waters. *Marine Chemistry* 101 (1–2), 130-140.
- 544 - Laglera, L.M., van den Berg, C.M.G., 2009. Evidence for geochemical control of iron by humic
545 substances in seawater. *Limnology and oceanography* 54, 610-619.
- 546 - Laglera, L.M., Downes, J., Santos-Echeandia, J., 2012. Comparison and combined use of non-linear
547 fitting for the estimation of complexing parameters from metal titrations of estuarine samples.
548 *Analytica Chimica Acta*, *submitted*.
- 549 - Leal, M.F.C., Vasconcelos, M.T.S.D., van den Berg, C.M.G., 1999. Copper induced release of complexing
550 ligands similar to thiols by *Emiliana huxleyi* in seawater cultures. *Limnology and Oceanography*
551 44, 1750-1762.
- 552 - Louis, Y., Garnier, C., Lenoble, V., Mounier, S., Cukrov, N., Omanovic, D., Pizeta, I., 2009. Kinetic and
553 equilibrium studies of copper-dissolved organic matter complexation in water column of the
554 stratified Krka River estuary (Croatia). *Marine Chemistry* 114, 110-119.
- 555 - Loureiro, J.M., 1979. Curvas de duração dos caudais medios diarios no rio Tejo. Technical Report,
556 Servico Hidraulico (DGRAH), Lisbon (1979).
- 557 - Mota, A.M., Cruz, P., Vilhena, C., Goncalves, M.L.S., 2005. Influence of the sediment on lead speciation
558 in the Tagus Estuary. *Water Research* 39, 1451-1460.
- 559 - Mucha , A.P., Almeida, C.M.R., Bordalo, A.A., Vasconcelos, M.T.S.D., 2010. LMWOA (low molecular
560 weight organic acid) exudation by salt marsh plants: Natural variation and response to Cu
561 contamination Estuarine, Coastal and Shelf Science 88, 63-70.
- 562 - Mucha , A.P., Almeida, C.M.R., Bordalo, A.A., Vasconcelos, M.T.S.D., 2008. Salt marsh plants (*Juncus*
563 *maritimus* and *Scirpus maritimus*) as sources of strong complexing ligands Estuarine, Coastal and
564 Shelf Science 77, 104-112.

- 565 - Pereira, P., Caçador, I., Vale, C., Caetano, M., Costa, A., 2007. Decomposition of belowground litter and
566 metal dynamics in salt marshes (Tagus Estuary, Portugal) *Science of the Total Environment* 380,
567 93-101.
- 568 - Pohl, C., Löffler, A., Hennings, U., 2004. A sediment trap flux study for trace metals under seasonal
569 aspects in the stratified Baltic Sea (Gotland Basin; 57°19.20' N; 20°03.00' E). *Marine Chemistry*
570 84, 143-160.
- 571 - Plavsic, M., Kwokal, Z., Strmecki, S., Peharec, Z., Omanovic, D., Branica, M. Determination of the copper
572 complexing ligands in the Krka rivers estuary. *Fresenius Environmental Bulletin* 18(3), 327-334.
- 573 - Quevauviller, P., Rauret, G., Rubio, R., Lopez-Sanchez, J.F., Ure, A., Bacon, J., Muntau, H., 1997.
574 Certified reference materials for the quality control of EDTA- and acetic acid-extractable contents
575 of trace elements in sewage sludge amended soils (CRMs 483 and 484). *Fresenius Journal of*
576 *Analytical Chemistry* 357, 611-618.
- 577 - Ruzic, I., 1982. Theoretical aspects of the direct titration of natural waters and its information yield for
578 trace metal speciation. *Analytica Chimica Acta* 140, 99-113.
- 579 - Santos-Echeandía, J., Laglera, L.M., Prego, R., van den Berg, C.M.G., 2008. Copper speciation in
580 estuarine waters by forward and reverse titrations. *Marine Chemistry* 108 (3-4), 148-158.
- 581 - Santos-Echeandía, J., Laglera, L.M., Prego, R., van den Berg, C.M.G., 2008. Dissolved copper speciation
582 behaviour during estuarine mixing in the San Simon Inlet (wet season, Galicia). Influence of
583 particulate matter. *Estuarine Coastal and Shelf Science* 76, 447-453.
- 584 - Santos-Echeandía, J., Prego, R., Cobelo-García, A., Millward, G.E., 2009. Porewater geochemistry in a
585 Galician Ria (NW Iberian Peninsula): implications for benthic fluxes of dissolved trace elements
586 (Co, Cu, Ni, Pb, V, Zn). *Marine Chemistry* 117, 77-87.
- 587 - Santos-Echeandía, J., Vale, C., Caetano, M., Pereira, P., Prego, R., 2010. Effect of tidal flooding on
588 metal distribution in pore waters of marsh sediments and its transport to water column (Tagus
589 estuary, Portugal) *Marine Environmental Research* 70, 358-367.

- 590 - Santos-Echeandía, J., Caetano, M., Brito, P., Canario, J., Vale, C., 2012. The relevance of defining trace
591 metal baselines in coastal waters at a regional scale: The case of the Portuguese coast (SW
592 Europe). *Marine Environmental Research*, in press.
- 593 - Shank, G.C., Skrabal, S.A., Whitehead, R.F., Kieber, R.J., 2004a. Strong copper complexation in an
594 organic-rich estuary: the importance of allochthonous dissolved organic matter. *Marine*
595 *Chemistry* 88, 21-39.
- 596 - Shank, G.C., Skrabal, S.A., Whitehead, R.F., Kieber, R.J., 2004b. Fluxes of strong Cu-complexing ligands
597 from sediments of an organic-rich estuary. *Estuarine Coastal and Shelf Science* 60 (2): 349-358.
- 598 - Skrabal, S.A., Donat, J.R., Burdige, D.J., 1997. Fluxes of copper-complexing ligands from estuarine
599 sediments. *Limnology and Oceanography* 42, 992-996.
- 600 - Skrabal, S.A., Donat, J.R., Burdige, D.J., 2000. Pore water distributions of dissolved copper and copper-
601 complexing ligands in estuarine and coastal marine sediments. *Geochimica et Cosmochimica Acta*
602 64, 1843-1857.
- 603 - Sundby, B., Vale, C., Caçador, I., Catarino, F., Madureira, M., Caetano, M., 1998. Metal-rich concretions
604 on the roots of salt marsh plants: Mechanism and rate of formation. *Limnology and*
605 *Oceanography* 43, 245-252.
- 606 - Turoczy, N.J., Sherwood, J.E., 1997. Modification of the van den Berg/ Ruzic method for the
607 investigation of complexation parameters of natural waters. *Analytica Chimica Acta* 354 (1-3),
608 15-21.
- 609 - Van den Berg, C.M.G., 1982. Determination of copper complexation with natural organic ligands in
610 seawater by equilibration with MnO₂ I. Theory. *Marine Chemistry* 11 (4), 307-322.
- 611 - Van den Berg, C.M.G. and Donat, J., 1992. Determination and data evaluation of copper complexation
612 by organic ligands in sea water using cathodic stripping voltammetry at varying detection
613 windows. *Analytica Chimica Acta* 257 (2), 281-291.

614 - Windom, H.L., Schropp, S.J., Calder, F.D., Ryan, J.D., Smith, R.G., Burney, L.C., Lewis, F.G., Rawlinson,
615 C.H., 1989. Natural trace metal concentrations in estuarine and coastal marine sediments of the
616 southeastern United States. *Environ. Sci. Technol.* 23, 314-320.

617 - Zwolsman, J.J.G., van Eck, G.T.M., 1999. Geochemistry of major elements and trace metals in
618 suspended matter of the Scheldt estuary, southwest Netherlands.
619 *Marine Chemistry* 66 (1-2), 91-111.

1 **Salt-marsh areas as copper complexing ligand sources to estuarine and coastal systems**

2 Juan SANTOS-ECHEANDÍA^{a,b,*}, Miguel CAETANO^a, Luis M. LAGLERA^c, Carlos VALE^a

3 ^a IPMA, Portuguese Institute of Sea and Atmosphere, Avenida Brasília 1446-006 Lisboa, Portugal

4 ^b Marine Biogeochemistry Group. Instituto de Investigaciones Marinas (CSIC). Vigo (Spain)

5 ^c University of Balearic Islands, Chemistry Department, Spain

6 *Corresponding author: jusae@iim.csic.es; tel. (+34) 986231930; fax(+34)986292762.

7 **Abstract**

8 Dissolved copper levels, copper complexing capacities and conditional stability constants have been
9 determined in the Tagus estuarine waters and one of the saltmarshes located in this estuary, the
10 Rosario saltmarsh. Tagus estuarine waters show a constant and around 20 nM copper concentration
11 during the estuarine mixing. Most of this copper is organically complexed by a strong ligand (L₁) with a
12 concentration that varies between 19-55 nM and a log K' between 14.14-15.75. In addition L₁/Cu ratios
13 are quite constants and close to 1 all through the estuary, indicating the same source. A second and
14 weakest ligand (L₂) was also detected in these waters in higher concentrations (36-368 nM) but with a
15 lower log K' that varies between 12.06-13.13. The present work has demonstrated that salt-marsh areas
16 are important and continuous sources of copper complexing ligands to the Tagus estuary. Noticeable,
17 tidal induced transport continuously feed these waters with copper and ligands, mainly with the
18 strongest one. This continuous input, together with the high residence times of this system results in a
19 quite constant concentration along the salinity gradient. This input represents 95% of the ligand present
20 in the estuary.

21 **Keywords:** copper; ligands; speciation; estuary; salt-marsh; Tagus

22 **1. INTRODUCTION**

23 Salt-marshes are among the most common and extensive intertidal habitats along temperate coastlines.
24 Several studies have shown that salt marshes incorporate large quantities of anthropogenic metals into
25 the colonized sediments (Caçador et al., 1993; Sundby et al., 1998; Caetano et al., 2007). Root-sediment

26 interactions appear to contribute to the metal enrichment of colonized sediments and belowground
27 biomass (Caçador et al., 1993) as well as porewaters (Santos-Echeandía et al., 2010).

28 Not only the concentrations, but also trace metals chemical forms in estuarine water (porewater and
29 water column) may control their bioavailability and toxicity. In the water column, speciation of many
30 biologically active trace metals is controlled by complexation with strong organic ligands (Bruland et al.,
31 1991). Copper (Cu) is probably the most studied metal in terms of organic complexation in seawater and
32 estuarine environments. This is because copper is a micronutrient, but it is also toxic, for example for
33 microalgae, at relatively low concentration levels. In addition, Cu forms complexes of relatively high
34 stability with various organic ligands. However, no many studies about copper complexation in salt-
35 marsh areas (Mucha et al., 2008) and its influence on the ligand budget of an estuary have been
36 published till these days.

37 Several sources of organic matter and ligands to estuarine and coastal areas have been pointed out in
38 the last years determining trace metal distribution along the salinity gradient (Laglera and van den Berg,
39 2003; Santos-Echeandía et al., 2008). In this way, autochthonous organisms are major producers of the
40 ligands that dominate the complexing capacity of open ocean and coastal productive waters (Croot et
41 al., 2000; Gordon et al., 2000). Organisms such as coccolithophores (Leal et al., 1999), cyanobacteria,
42 dinoflagellates (Croot et al., 2000) and heterotrophic bacteria (Gordon et al., 2000) have been observed
43 to excrete strong Cu-complexing ligands, most likely as a defense mechanism against metal toxicity. The
44 input of terrestrial humic substances through riverine waters has also been recognized as an important
45 source of strong ligands to estuarine environments (Kogut and Voelker, 2001; Shank et al., 2004a;
46 Laglera et al., 2009).

47 Recent studies have shown that estuarine sediments can also act as a significant source of Cu-
48 complexing ligands to the overlying water, which may strongly influence the biogeochemistry and
49 cycling of dissolved Cu by sediment/water exchange (Skrabal et al., 1997, 2000; Shank et al., 2004b,
50 Chapman et al., 2009). This source of organic ligands would be enhanced if sediments are colonized by
51 plants (Mucha et al., 2008). In the last years, several studies conducted in salt marsh areas, have shown
52 that as roots die they supply important quantities of organic matter to the sediment (Caçador et al.,
53 2004; Pereira et al., 2007). In addition, low molecular weight organic acids are exudated by salt-marsh

54 plant roots (Mucha et al., 2010) that can bind and redistribute metals (Mucha et al., 2008) due to their
55 high affinity to organic matter.

56 As tidal water floods the salt marsh, large quantities of organic material, nutrients and trace metals
57 accumulated in the area are exported to the estuary. On a semidiurnal tidal scale, advective fluxes are
58 enhanced in salt marsh sediments (Santos-Echeandía et al., 2010) through a mosaic of small channels in
59 the upper sediments. The relevance of the tidal induced transport on copper and complexing ligands
60 may be crucial to understand the biogeochemical cycles of metals in coastal ecosystems where salt-
61 marshes occupy large extensions.

62 Thus, the objectives of this work are: a) to measure dissolved copper and complexing ligand
63 concentrations in the Tagus estuarine waters b) to determine dissolved copper and complexing ligand
64 concentrations in the Rosário salt-marsh flooding and porewaters c) to estimate dissolved copper and
65 ligand advective fluxes in the Rosário saltmarsh d) to ascertain the importance of this input over the
66 Tagus estuarine waters.

67 **2. MATERIAL AND METHODS**

68 *2.1. Study area*

69 The 340 km² of the Tagus estuary represent one of the largest transitional systems in Europe. The
70 estuary is composed by a large shallow inner bay and a deep straight and narrow inlet channel (Fig. 1).
71 This channel reaches a depth of 40 m and constitutes the deepest part of the estuary. The bay has a
72 complex bottom topography with channels, tidal flats and islands. The deepest channel, with a water
73 depth of 5-10 m, is an extension of the inlet channel. The total amount of water in the estuary is around
74 1.9 km³. The southern and eastern parts of the bay contain extensive inter-tidal mudflats; the northern
75 part contains tidal flats, islands and several smaller channels. These channels merge upstream to a single
76 narrow channel, marking the entrance of the Tagus River.

77 The Tagus River is the main source of freshwater to the estuary. The discharge usually shows a
78 pronounced dry season/wet season as well as large inter-annual variation. The average annual discharge
79 is ~400 m³ s⁻¹, but seasonally the average monthly discharge may vary from 1 m³ s⁻¹ to > 2200 m³ s⁻¹
80 (Loureiro, 1979). Consequently, the residence time of freshwater in the estuary is highly variable and

81 may range seasonally from 6 to 65 days (Braunschweig et al., 2003). The tides are semi-diurnal, with
82 amplitudes at Lisbon ranging from ~ 1 m at neap tide to ~ 4 m at spring tide. The tidal effect reaches 80
83 km landward of the estuary mouth. Most pollutants are discharged from upper to the lower estuary (Fig.
84 1). Indeed, apart from being a major harbor, the fishing activities in the estuary are adversely affected
85 by the inflow of effluents from about 3.5 million Greater Lisbon inhabitants, part of them untreated,
86 coupled with industrial (chemicals and petrochemicals) and agricultural (fertilizers and pesticides)
87 contributions.

88 Almost 40% of the estuary is composed by inter-tidal mudflats mainly in southern and eastern shores,
89 containing extensive areas of salt marshes colonised mainly by *Sarcocornia fruticosa*, *Sarcocornia*
90 *perennis*, *Halimione portulacoides* and *Spartina maritima* occupying an area around 20 km². The marsh
91 selected for this study (Rosário) is located in the southern shoreline of the estuary (Fig.1). It covers an
92 area of 2 km² (Crespo, 1993), being characterised by homogeneous stands of *S. maritima* as a pioneer
93 species in the lower part, pure stands of *H. portulacoides* across the 20-50 cm elevation transect, and *S.*
94 *fruticosa* and *S. perennis* in the higher salt marsh. The marsh is fully inundated twice a day by tidal action
95 (2-4 m of tidal amplitude) through a highly branched system of channels that cross the elevation
96 transect. The channels have 0.5-1.5 m depth promoting the inundation of the higher marsh even at low
97 amplitude tides.

98 2.2. Sampling

99 A sampling cruise along the Tagus estuary was conducted on the 5th May 2010. A 93 m³ s⁻¹ flow was
100 measured during that day what gives a residence time around 62 days for the water in the estuary
101 (Braunschweig et al., 2003). Ten sub-surface water samples (TWB11-TWB410) were collected by hand in
102 1 L low density polyethylene (LDPE) bottles from a plastic boat (Fig. 1) during the low tide covering the
103 salinity gradient of the estuary. In addition, flooding water during tidal inundation was sampled in two
104 sites of the Rosário salt marsh (non-vegetated area and *S.maritima* colonised area and separated by less
105 than 20 m). At low tide, when sediment was exposed to the atmosphere, two sediment cores (10 cm
106 long) were collected at each site (vegetated and non-vegetated). The cores were sliced immediately
107 after sampling in two 4 cm layers, prepared composite samples for each layer of the cores collected at
108 each site, and material stored in acid pre-cleaned HDPE vials avoiding air presence inside. Sampling took

109 place in less than 3 min. Core material in the colonized area consisted of dense rooting sediments with
110 no evidence of burrowing worms, crabs or bivalves. When tidal water starts to flood each site, flooding
111 water was collected at each inundation time: 1, 5, 10, 15, 20 and 30 min for the non-vegetated area and
112 1, 5, 10, 15, 20, 30, 45 and 85 min for plant colonized area. Flooding water was sampled 1 cm above the
113 sediment surface directly into acid pre-cleaned syringes. The water and sediment samples were kept in
114 refrigerated boxes and immediately transported to the laboratory. A more detailed description of these
115 sampling procedures can be found in previous works (Caetano et al., 2007).

116 *2.3. Sample treatment*

117 Estuarine and flooding water samples were filtered through 0.45 μm cellulose membranes placed in
118 previously acid-cleaned filtration units (Nalgene). Filters were frozen and stored at -20°C pending
119 analysis of particulate copper and aluminium. The main reason for measuring particulate aluminium is
120 that it acts as a tracer of lithogenic or terrigenous material (Windom et al., 1989; Pohl et al., 2004) and
121 will be useful for the interpretation of the various sources of material to estuarine waters (i.e. rivers or
122 sediment resuspension) (Mota et al., 2005).

123 Pore waters were separated from the sediment layers by centrifugation at 10,160 rcf \times g for 30 min at $+4$
124 $^{\circ}\text{C}$ and filtered through 0.45 μm cellulose acetate membranes. Filtration and subsequent manipulation
125 of the samples were carried out in a glove box under argon atmosphere in order to avoid alteration of
126 the initial conditions (Caetano et al., 2007; Santos-Echeandia et al., 2009). A portion of the filtered
127 samples (around 200 mL) was frozen for speciation analysis while around 100 mL were acidified with
128 suprapure HCl ($\text{pH} < 2$) and stored pending analysis of total dissolved copper.

129 *2.4. Copper analysis in estuarine water*

130 *2.4.1. Total dissolved copper concentrations*

131 Copper analyses were carried out using voltammetric equipment (Metrohm 797 VA Computrace)
132 controlled by a computer (PC). The reference electrode was a double junction, Ag/AgCl, KCl (3 M),
133 saturated AgCl, with a salt-bridge filled with 3 M KCl, and the counter electrode was a glassy carbon rod.
134 A hanging mercury drop electrode (HMDE) was used as the working electrode. The copper
135 concentration in the filtered samples was determined using a procedure similar to the one described

136 previously (Campos and van den Berg, 1994). Estuarine and flooding water was UV-digested (1 h) after
137 acidification to pH 2.2 by the addition of 10 μ L 6 M bidistilled HCl (AnalR BDH) per 10 mL of sample in
138 acid-cleaned borosilicate glass tubes. A 10 mL sample aliquot was pipetted into the voltammetric cell
139 and ammonia (AristarGrade Merck) was used to ascertain the approximate neutralization of the pH;
140 also, HEPES buffer (BDH, final concentration 0.01 M) and Salycildoxime (SA, Sigma, final concentration of
141 25 μ M SA) were added. The solution was deaerated by purging (5 min) with nitrogen. The voltammetric
142 parameters were: deposition 60 s at -1.1 V whilst stirring, 8 s quiescence at -0.1 V, and a potential scan
143 using the square-wave modulation: 10 Hz, step height 2.5 mV, pulse height 25 mV, from 0 to -0.8 V. The
144 sensitivity was calibrated by incorporating standard copper additions (Spectrosol BDH) to each sample.
145 Each sample was analyzed in triplicate. A blank with Milli-Q water (18.2 M Ω .cm) was made at intervals
146 of every three samples and its concentration was subtracted in order to eliminate any copper
147 contribution from reagents. Blank concentrations were around 0.27 \pm 0.06 nM.

148

149 *2.4.2. Copper titrations*

150 The copper complexing capacity of the waters of the Tagus estuary was determined by competing ligand
151 exchange with adsorptive cathodic stripping voltammetry (CLE-AdCSV) of Cu-salycilaldoxime (SA)
152 complexes according to previous works on copper complexation in estuarine waters (Campos and van
153 den Berg, 1994; Laglera and Van Den Berg, 2003). Briefly, a 170-ml sample previously filtered by 0.45 μ m
154 was transferred to a polyethylene bottle (Nalgene), and spiked with HEPES/NH₄OH buffer (for a
155 concentration of 0.01 M) and SA (mix concentration of 5 or 10 μ M). After stirring, 10 mL aliquots were
156 pipetted into 15 polystyrene vials (30 mL Bibby, Sterilin) that were previously spiked with copper to
157 provide increasing concentrations in the range of 0–700 nM (actual range depending on the initial
158 copper concentration and the ligand concentration to be determined). Prior to the first titration, the
159 tubes were conditioned twice overnight with seawater containing the same range of copper
160 concentrations in order to avoid copper loss in the tube walls. After that, aliquots of each sample were
161 left to equilibrate overnight at room temperature due to the slow kinetics of the ligands and copper
162 reactions (Campos and van den Berg, 1994). The equilibrium concentration of Cu-SA complexes was
163 determined using the following parameters: adsorption potential of -0.15 V, deposition time of 60 s, 8 s

164 quiescence, potential scan from 0 to -0.8 V using square-wave modulation at 10 Hz, step height 2.5mV
165 and pulse height of 25 mV.

166 2.4.3. Evaluation of complexing capacities and conditional stability constants

167 Changes in the ratio between the concentrations of CuSA (labile to AdCSV) and CuL in the different
168 aliquots permit the determination of the copper complexing capacity of the ligands present in solution
169 (C_L) and their conditional stability constant to bind copper (K'_{CuL}). A more detailed explanation can be
170 found elsewhere (Ruzic, 1982; van den Berg, 1982). The relationship between the different copper
171 fractions is described by the following transformation of the Langmuir isotherm:

$$172 \quad [Cu]_{TOT} = \sum (C_{Li} [Cu]_{lab} / K'_{CuLi\alpha'} + [Cu]_{lab}) + [Cu]_{lab} \quad (1)$$

173 L_i represents the variability of the nature of the different natural ligands. Those ligands are
174 differentiated according to the stability of their complexes with copper. α' is the α -coefficient of Cu^{2+}
175 with inorganic ligands and SA. $[Cu]_{TOT}$ and $[Cu]_{lab}$ are respectively the total and labile copper
176 concentrations related by:

$$177 \quad [Cu]_{TOT} = \sum [CuLi] + [Cu]_{lab} = \sum [CuLi] + [Cu(SA)] + [Cu(SA)_2] \quad (2)$$

178 The concentration of labile copper is calculated from:

$$179 \quad [Cu]_{lab} = i_p / S \quad (3)$$

180 Where i_p is the voltammetric signal obtained from the reduction of the CuSA complexes adsorbed on the
181 HMDE electrode and S is the ratio signal/concentration or sensitivity. S can be estimated from the slope
182 of the last few points of the titration (S^{INT}) if the titration has been extended to copper concentrations
183 enough to complete the saturation of the natural ligands.

184 As indicated in the previous section, samples were analyzed using two different SA concentrations (5
185 and 10 μ M). Higher SA concentrations increase the competing ability of SA. In the presence of complex
186 mixes of ligands characterized by the formation of complexes with copper in a wide range of stability
187 constants, the effect of increasing the SA concentration is both, an overcompetition of those ligands of
188 low affinity for copper and the equilibration of SA with ligands of very high stability constant. Therefore,
189 in heterogeneous matrices, the shift of the SA concentration resolves a different fraction of ligands,

190 fraction that is defined as detection window. This is an important tool to estimate the heterogeneity of
191 the pool of copper ligands in the sample.

192 Values for the stability constants of the complexes CuSA and Cu(SA)_2 are necessary in order to obtain
193 the value of α' at each salinity. Both stability constant were calculated using relationships obtained in a
194 previous work (Campos and van den Berg, 1994):

$$195 \quad \log K_{\text{CuSA}} = (10.12 \pm 0.03) - (0.37 \pm 0.02) \log \text{salinity} \quad (4)$$

$$196 \quad \log \beta'_{\text{Cu(SA)}_2} = (15.78 \pm 0.08) - (0.53 \pm 0.07) \log \text{salinity}. \quad (5)$$

197 A plot of $[\text{Cu}]_{\text{lab}}$ vs the ratio $[\text{Cu}]_{\text{lab}}/[\text{CuL}]$ is the most used procedure to solve C_L and K'_{CuL} from the slope
198 and the Y-axis value respectively. When only one ligand is present, the data follow a straight line but if
199 more than one type of ligands are present, the plot takes a curved shape. In this case C_L and K'_{CuL} can be
200 calculated with accuracy for a maximum of two types of ligands.

201 The estimation of C_{L1} , K'_{CuL1} , C_{L2} and K'_{CuL2} requires either an iterative refine procedure (Laglera-Baquer et
202 al., 2001; van den Berg, 1982) or a nonlinear fitting (Gerringa et al., 1995). In the first case the solutions
203 for C_{L1} and K'_{CuL1} are refined with estimations of C_{L2} and K'_{CuL2} from different linear sections of the plot
204 until a convergent solution is obtained.

205 Complexing capacities, conditional stability constants and S can also be obtained fitting non-linearly the
206 substitution of Eq(3) in Eq(1). Non-linear fitting prevents the uncertainty caused by the arbitrary
207 necessity to split the titration data in two that iterative linear fitting requires.

208 In this work, we have used the fitting tool of a popular computer program, SigmaPlot (© Systat
209 Software, Inc) to fit 3, 4 or 5 parameters. The program uses a Levenberg-Marquardt fitting algorithm.
210 We first solved the titration data sets for the hypothesis of a single ligand model using non-linear fitting
211 incorporating S as a parameter to C_L and K. For this purpose, a new equation was incorporated to the
212 Regression Wizard of the software under the "User-Defined" category. The Code fed to the Regression
213 Wizard is presented in Table S1.

214 Then, we prepared a new Equation for the case of two types of ligands, i.e. 5 parameters (C_{L1} , K'_{CuL1} , C_{L2}
215 and K'_{CuL2} and S) but the program struggled to offer realistic values in the form of very high S and K'_{CuL1}
216 values. Removal of S from the list of parameters and use of S^{INT} did not solve problems with K'_{CuL1} for

217 some titrations. In those cases, K'_{CuL1} was obtained from the iterative linear routine and its value fixed in
218 the *constrains* section of the code (Table S1) during the non-linear fitting of the rest of the complexing
219 parameters.

220 2.4.4. Particulate copper and aluminum

221 In order to determine the amount of labile copper, filters obtained from filtered water were subject to
222 digestion overnight with 0.1 M acetic acid in Teflon® vials (Savillex) at ambient temperature following
223 the first step of the BCR extraction procedure (European Community Bureau of Reference; Quevauviller
224 et al., 1997). The digest was then syringed-filtered (0.45 μm) using a Swinnex filtration unit and stored
225 pending analysis; filters containing the remnant particles were microwave digested using a mixture of
226 HF and HNO_3 (1:3) in order to analyze the total fraction (Biscombe, 2004).

227 Labile copper determination was carried out by means of cathodic stripping voltammetry as explained
228 before (Campos and van den Berg, 1994) while total particulate copper and aluminum determination
229 was carried out with the standard additions method. Concentrations of Al and Cu were determined
230 using a quadrupole ICP-MS (Thermo Elemental, X-Series) equipped with a Peltier Impact bead spray
231 chamber and a concentric Meinhard nebulizer. Coefficients of variation for metal counts ($n = 5$) varied
232 between 0.5 and 2%. The precision and accuracy of each metal concentration measurements,
233 determined through repeated analysis of certified reference material (PACS2), using Indium as internal
234 standard, were 1–4% and 2–5%, respectively (data not shown). Procedural blanks always accounted for
235 less than 1% of the total metal concentrations in samples.

236 2.5. Estimation of sediment-water interchange: tidal induced fluxes

237 As water floods over inter-tidal sediments the pore water solutes tend to be exported by advection
238 and/or exchanged between mixing top sediments and tidal water. The associated pressure difference
239 and tidal water movement are the driven mechanism for this transport. By using the temporal variation
240 of copper and ligand concentrations in the flooding water the tidal induce transport (T) to the water
241 column is calculated using the following expression (Caetano et al., 2007).

$$242 \quad T = \sum [(C_{t+1} - C_t)/(2 - C_i)](h_{t+1} - h_t) \quad (6)$$

243 where C_{t+1} and C_t are solute (copper and ligand) concentrations in the flooding water at times $t+1$ and t ,
244 C_i is the residual concentration (lowest value obtained for the flooding water) and h_t and h_{t+1} are the
245 water depth at the same times. It was observed that water depth during the field measurements
246 increased on the average 0.5 and 0.8 cm per minute of inundation in *S. maritima* and non-vegetated
247 areas, respectively. The tidal induced transport of trace metals is calculated for the first 85 and 30 min
248 of inundation, respectively. Since inter-tidal sediments are inundated twice a day, the tidal induce
249 transport (T) was multiplied by a factor of two to present values on a daily basis.

250 2.5. Statistics

251 The statistical analyses were performed using STATISTICA 6 (Statsoft).

252 3. RESULTS

253 3.1. Determination of the complexing parameters and the sensitivity by non-linear fitting

254 Table 1 shows the complexing parameters found for the estuarine water samples according to one and
255 two ligands models. Table 2 shows those parameters for flooding waters and interstitial waters
256 extracted from cores. For the one ligand model, S was added to the fitting procedure according to the
257 code shown in Table S1. Values for S were in the range 94-113 % with respect to S^{INT} (average 98.9 ± 4.1
258 %) indicating that any bias due to undersaturation of the ligands present in the sample caused by a too
259 small copper concentration at the end of the titration was masked by the analytical error. For the
260 sample collected at station 11, S was fitted at a very low value 90% of S^{INT} and the complexing
261 parameters were recalculated using S^{INT} .

262 For the two ligands model, this approach was not possible as explained above. For some titration sets, S
263 was estimated to be 103-114 % of S^{INT} but for many others this correction reached as much as 170 %
264 which could be discarded simply by visual inspection. Values in Table 2 were obtained using S^{INT} . When
265 the estimation of K'_{CuL1} produced a value over 20, the titration data set was solved by iterative linear
266 fitting (Laglera-Baquer et al., 2001; Laglera and Van Den Berg, 2003) and the value of K'_{CuL1} fixed on the
267 constrains section of the code. This led to a 3 parameters non-linear fitting. An extensive description of
268 the routine to fit complexing parameters out of metal titration data sets used here is presented in a
269 separate work (Laglera et al., 2012).

270 3.2. Dissolved copper and its organic speciation in the Tagus estuary

271 Dissolved copper concentrations along the salinity gradient in the Tagus estuary are plotted in Fig. 2a.
272 With the exception of the station located upstream in the river (26.4 nM), values were quite constants
273 and around 20 nM all over the estuary. The ligand concentration (L ; Fig. 2a), for the 5 μ M SA detection
274 window, showed higher values in riverine samples (399 nM) decreasing to 320-340 nM in the first 3
275 units of salinity. A new decay is found from salinity 5 to 25 (to 46 nM). This decreasing trend from fresh
276 to marine waters has been observed before in other estuarine systems (Laglera et al., 2003; Plavsic et
277 al., 2009). The conditional stability constant for these ligands ($\log K'$) ranges between 12.20 and 13.26
278 (Table 1), and it presents a bowl-shape distribution along the salinity gradient, with lower values in the
279 mid-estuary and maxima at marine (13.26) and riverine (13.11) end-members.

280 By fitting data to two types of ligands, a strong (L_1) and a weak (L_2) one can be observed in the Tagus
281 estuary waters (Fig. 2a). Ligand L_1 varied between 14 and 55 nM being the highest concentration found
282 in the two most riverine stations. Values decreased sharply to 15 nM at salinity 3 remaining almost
283 constant until the marine end member (salinity 25). Otherwise, L_2 concentrations vary between 36 and
284 368 nM with a conservative distribution between salinities 5 and 25, but with lower values than
285 expected for an ideal dilution line between salinities 0 and 5. The conditional stability constants for
286 these ligands range between 14.10 and 15.75 for L_1 and between 12.06 and 13.13 for L_2 (Table1). The
287 distribution along the salinity gradient is different among them; while $\log K_1'$ shows a saw tooth
288 tendency with higher values in the riverine end-member, $\log K_2'$ distribution is comparable to $\log K'$,
289 with the lowest values in the mid estuary and increasing towards the river (13.13) or the sea (12.42) end
290 members.

291 In order to detect stronger copper complexing ligands and check for homogeneity/heterogeneity of
292 them in the estuary (van den Berg and Donat, 1992; Buck and Bruland., 2005; Santos-Echeandia et al.,
293 2008), a detection window of 10 μ M SA has been applied to some of the samples. Samples, fitted to one
294 ligand are plotted in Fig. 2b. Ligand concentration increases between salinity 0 and 5 (from 121 to 142
295 nM) and progressively decreases to 30 nM at salinity 25 with a quite linear trend. The conditional
296 stability constant ($\log K'$) presented, again, lower values at mid salinities (13.11) increasing towards the
297 riverine (14.52) and marine (13.76-14.15) end members (Table 1) as observed for the lower detection

298 window (5 μM SA). By fitting data to two types of ligands, the strongest one (L_1) concentrations ranged
299 between 15 and 28 nM (Fig. 2b) with a quite irregular distribution. On the contrary, the weakest ligand
300 of this detection window (L_2) shows a similar trend to L_1 , with an initial increase from 145 to 174 nM
301 decreasing progressively afterwards to 22 nM at salinity 25. The conditional stability constants, both \log
302 K_1' and $\log K_2'$ present higher values at low salinities (16.84 for K_1 and 13.87 for K_2) that sharply
303 decreased at salinity 5 reaching 15.02 for $\log K_1'$ and 12.76 for $\log K_2'$ remaining relatively constant
304 towards the marine end-member (Table 1).

305 *3.3. Suspended Particulate Matter, particulate total and labile copper and aluminium concentrations in* 306 *the Tagus estuary*

307 Suspended particulate matter values oscillate between 4.8-14.7 mg L^{-1} in the estuary with an irregular
308 distribution (Fig. S1a). The highest values were found at salinities 10-15 and the lowest between
309 salinities 19-23. Particulate copper concentrations varied between 0.78 and 14.8 nM (Fig. S1b). The
310 highest levels were found at mid-salinities (5-15 ups) while the lowest values measured at both end-
311 members. The labile copper in the particulate matter accounts only for the 0.05-0.45 % of the total
312 copper but it is noticeable that the lability was higher for the lowest salinities (Fig. S1c). Particulate
313 aluminum concentrations ranged between 272 and 4930 nM with a similar distribution to particulate
314 copper.

315 *3.4. Dissolved copper and its organic speciation in the Rosario Saltmarsh*

316 *3.4.1. Flooding waters*

317 Dissolved copper concentrations in the flooding water in the two sites of the salt marsh (non-vegetated
318 and plant colonized areas) are plotted in Fig. 3a. Copper levels in the non-vegetated zone increase 1
319 minute after arriving of tide water from 18.3 to 28.5 nM. In the following 5 minutes, levels decreased
320 reaching 20.6 nM and remaining quite constant until 30 minutes after tidal inundation started, with the
321 exception of minute 15 when a less pronounced increase (27.0 nM) was observed (Fig. 3a). In a similar
322 way, dissolved copper levels increased in the colonized area 1 minute after the flood started reaching
323 higher values (32.5 nM) than in the non-vegetated area. Afterwards, concentrations decreased to 17.7
324 nM and varied irregularly between 13.6 and 22.1 nM during the next 80 minutes of inundation.

325 The time course evolution of ligand concentration in the flooding waters is also plotted in Fig. 3a. A net
326 increase of its concentration (initial levels of 46 nM) was observed in both sampling areas but reaching
327 higher concentrations in the plant colonized (291 nM) than in the non-vegetated area (85 nM) during
328 the first minute of inundation. Afterwards levels in plant colonized sediments decreased sharply while in
329 non-vegetated area values diminished progressively reaching, at both areas similar values to those
330 found before inundation started. The conditional stability constants of ligand showed higher values in
331 the non-vegetated (13.73-14.04) than in the plant colonized area (13.11-13.89) (Table 2). The
332 significance for statistical analyses was $p < 0.05$.

333 In addition, the time course evolution of $\log K'$ values during the tidal inundation were different among
334 the two sites: while an increase of $\log K'$ was found one minute after the inundation started in the non-
335 vegetated area, a progressive increase of $\log K'$ with time was observed in the vegetated area during the
336 first 10 minutes.

337 The strongest ligand (L_1) concentrations vary between 46 and 61 nM in the non-vegetated area without
338 a trend all over the time (Fig. 3b). Nevertheless, L_1 concentrations in the colonized area are more
339 variable and ranged between 28 and 95 nM. The conditional stability constant of this ligand varied
340 between 14.12 and 14.79 in the non-vegetated area while in the colonized area a variation between
341 13.61 and 14.83 was found (Table 2). The weakest ligand concentrations were higher and varied
342 between 60 and 107 nM for the non-vegetated area and from 5.5 to 258 nM for the colonized area (Fig.
343 3b). It is noticeable the net increase in the colonized area in the first minutes of inundation that is not
344 observed in the non-vegetated area. Finally, conditionals stability constant for this weakest ligand
345 oscillate between 11.95-12.26 nM in the non-vegetated area and 11.87-13.05 in the colonized area
346 (Table 2).

347 Strongest ligands have been detected in the flooding waters moving the detection window to 10 μ M SA.
348 Ligand concentration were lower (61-87 nM) in the non-vegetated area than in the colonized site (107-
349 137 nM) during the first 5 minutes of inundation (Fig. 3c). An increase was found in the first minute
350 comparing to the estuarine waters in the vicinity of the salt-marsh and concentrations slightly decrease
351 after 5 minutes. The respective conditional stability constants were similar in the non-vegetated area
352 (14.39-14.48 nM) and in the plant-colonized area (14.32-14.47 nM) (Table 2).

353 Two types of strong ligands were found in the colonized area with concentrations ranging between 58
354 and 82 nM for L_1 and from 59 to 138 nM for L_2 with a similar trend to the unique ligand (L). However, L_1
355 levels do not decrease after 5 minutes but continue to increase (Fig. 3c). Conditional stability constants
356 ranged in the following intervals: 14.63-15.69 for L_1 ; and 12.84-13.44 for L_2 (Table 2).

357 3.4.2. Porewaters.

358 Dissolved copper and ligand concentrations and their conditional stability constants in the porewaters of
359 the salt-marsh are shown in Table 3. Levels of dissolved copper in the non-vegetated area ranged from
360 45.3 to 53.9 nM with higher values in the upper layer than in the deeper one. However, higher ligand
361 concentrations were found in deeper porewaters (321 nM) than in surface ones (245 nM). The
362 conditional stability constants for these ligands varied between 13.24 for the deeper layer and 13.58 for
363 the upper one. Levels of the stronger ligand (L_1) ranged from 77 to 184 nM with higher values in the
364 upper layer. Nevertheless, the conditional stability constant was higher (14.77) in the deeper layer than
365 in the upper one (13.70). Concentrations of L_2 varied between 70 and 287 nM with increased values in
366 the deeper layer. The conditional stability constants of this weakest ligand were 12.68 for the deeper
367 layer and 13.09 for the upper one.

368 Higher dissolved copper concentrations in pore waters (71-142 nM) were found in the plant colonized
369 area (Table 3). Ligand concentrations vary between 767 nM in the deeper layer and 831 nM in the upper
370 one. Conditional stability constant for this ligand showed higher values in the upper layer. The stronger
371 ligand, L_1 , levels varied between 115 and 203 nM with higher values in the upper layer and their
372 conditional stability constants were 15.17 for the upper layer and 14.66 for the deeper one.
373 Concentrations of L_2 were quite similar among layers (666 and 699 nM) as the conditional stability
374 constants (13.09 and 12.82).

375 Strongest ligands in pore waters were found by applying a higher detection window (10 μ M) (Table 3).
376 Ligand concentration in the non-colonized area was 230 nM with a conditional stability constant of
377 14.28. A strong ligand with a $\log K_1'$ of 15.25 and a concentration of 67 nM and a weak ligand with a \log
378 K_2' of 13.85 and a concentration of 182 nM result from the data fitting to two types of ligands. As found
379 with the 5 μ M SA detection window, higher values were observed in the vegetated area at 10 μ M
380 detection window. A ligand concentration of 419 nM with a $\log K'$ of 13.95 was registered. In the data

381 fitting to two types of ligands, a strong ligand concentration of 148 nM with a log K_1' of 17.56 was
382 recorded, while the weakest ligand showed a concentration of 846 with a log K_2' of 13.51.

383 *3.5. Tidal induced transport of copper and organic ligands in the Rosario Saltmarsh*

384 An estimation of the tidal induced transport of dissolved copper and ligands is shown in Table 4. A flux
385 of $1.23 \mu\text{mol m}^{-2} \text{d}^{-1}$ of dissolved copper escapes from the sediment to the overlying waters in the non-
386 vegetated area, while the ligand transport was $3.25 \mu\text{mol m}^{-2} \text{d}^{-1}$. If the two ligand case is considered, an
387 export of $2.16 \mu\text{mol m}^{-2} \text{d}^{-1}$ of the strongest ligand and $2.31 \mu\text{mol m}^{-2} \text{d}^{-1}$ of the weakest one was
388 estimated. As expected from the results shown in previous sections calculated transports are higher in
389 the plant colonized area, where a $2.43 \mu\text{mol m}^{-2} \text{d}^{-1}$ flux of dissolved copper is estimated. The ligand flux
390 ($48.2 \mu\text{mol m}^{-2} \text{d}^{-1}$) was around fifteen times higher than in the non-vegetated area. Increased transport
391 of both strong and weak ligand to the water column was also found with $11.5 \mu\text{mol m}^{-2} \text{d}^{-1}$ for L_1 and
392 $64.7 \mu\text{mol m}^{-2} \text{d}^{-1}$ for L_2 .

393 The tidal induced transport of ligands detected by the 10 μM SA detection window was similar in the
394 non-vegetated area and lower in the colonized area. In this way, $4.25 \mu\text{mol m}^{-2} \text{d}^{-1}$ of ligands were
395 exported in the non-colonized area while $6.87 \mu\text{mol m}^{-2} \text{d}^{-1}$ were exported in the plant colonized area.
396 For the two ligand case, $3.80 \mu\text{mol m}^{-2} \text{d}^{-1}$ of the strongest ligand and $5.77 \mu\text{mol m}^{-2} \text{d}^{-1}$ of the weakest
397 one were estimated.

398 **4. DISCUSSION**

399 *4.1. Copper and organic ligands behavior during the estuarine mixing*

400 Dissolved copper and complexing ligand behavior in the Tagus estuary can be clearly divided in two
401 distinct chemical areas. The edge is marked by the salinity 5.6 sample. In the low salinity stretch,
402 although dissolved copper values were only higher in the most riverine sample, the strong ligand values
403 (L_1) were higher than in the rest of the estuary. As a consequence the L_1/Cu ratio is relatively constant
404 and around 1. The only exceptions are the two most riverine stations (Fig. S2) where an excess of L_1 ,
405 which may derived from the river end member was detected. This ratio is linear and progressively
406 decreases with the increasing salinity if total ligand concentration is considered (Fig. S2). Moreover, the
407 weakest ligand (L_2) also showed a different behavior in this zone of the estuary but with lower levels

408 than expected if the trend marked by the seven most saline stations is extended to the freshwater end-
409 member.

410 The mixing of freshwater with the marine water dilutes L_1 ligand within the estuarine area. The long
411 residence times (Braunschweig et al., 2003), confirmed by uniform suspended particulate matter
412 content in a wide salinity range (Fig. S1a), allow the homogenization of the water body justifying the
413 constancy of copper and strong ligand levels in the 6-25 salinity range. This pattern suggest that the tidal
414 effect superimposes the river flow and no losses of copper or strong ligands occurred during the
415 estuarine mixing. Similar findings have been observed in the Scheldt estuary by Laglera and van den
416 Berg (2003). A continuous lateral input, as detected in the Vigo Ria (Santos-Echeandía et al., 2008), in
417 the Tagus estuary may also explain the constant values all over the salinity gradient. In addition, this
418 area shows constant and close to the unit L_1/Cu ratios in a wide salinity range (Fig. S2). This means that
419 copper and L_1 levels are similar probably because their source is the same. There is no evidence of
420 copper transfer from the dissolved to the particulate fraction since values were quite low all through the
421 estuary (Fig. S1b). However, L_2 experiments a progressive decrease in their levels towards the outer part
422 of the estuary and no remarkable inputs of L_2 are observed at mid-high salinities as observed for L_1 . It
423 can be assumed that the river is not the major source of this weak ligand, but its origin is somewhere in
424 between salinities 0-6, where although the mixing with seawater, its concentration remains constant or
425 even increases. This increase is consistent with the trend observed at both detection windows for the
426 weakest ligand (Fig. 2). The higher particulate aluminum concentrations at salinities 6-10 (Fig. S1c) and
427 SPM at salinity 10 could reflect the maximum turbidity zone in this salinity gradient and at spring tides
428 the bottom particle resuspension in this area may explain the release of the weakest ligand from the
429 sediments (Shank et al., 2004; Santos-Echeandia et al., 2008). If copper variability during the estuarine
430 mixing is associated to L_1 , L behavior is ruled by L_2 . This fact is supported by the spatial distribution of log
431 K'_2 , which is quite similar to log K' (Table 1) at both detection windows (5 μM y 10 μM).

432 Regarding the nature of the ligands, by comparing L_1 with L_2 at both detection windows, the distribution
433 of the stronger ligand (L_1) was homogeneous, mainly at high salinities, because the log $K'_{1,5\mu MSA}$ and log
434 $K'_{1,10\mu MSA}$ were similar (Table 1) and, in general, their ratio was close to 1 (Fig.S3a). Moreover, ratios
435 between L_1 measured at the low detection window and the L_1 observed at the high detection window

436 were closer to 1 (1.24 ± 0.33) along the salinity gradient (Fig.S3b). Conversely, L_2 was very heterogeneous
437 and a shift to the higher detection window induces the decrease of the ligand concentrations. Thus, the
438 ratio between L_2 measured at low detection window and at high detection window is around 2
439 (2.09 ± 0.48) (Fig. S3b). An increase of the log K' values is also observed when moving the detection
440 window to 10 μM SA. As a consequence the ratios between log K' at high and low detection windows are
441 always well below 1 all over the salinity gradient (Fig. S3a).

442 *4.2. Saltmarsh inputs of copper and complexing ligands to the estuary*

443 Intertidal and saltmarsh areas constitute one of the possible sources of copper and complexing ligands
444 to estuarine waters. Mucha et al. (2008) demonstrated that salt-marsh plants are able to produce
445 relatively high amounts of strong Cu-complexing ligands in their root system and the present study
446 evidenced that these complexes are exported to estuarine waters through tidal induced transport (Table
447 4).

448 The constant dissolved copper and L_1 concentrations in a wide salinity gradient (6-25) is presumably
449 explained by the lateral input from the marsh areas along the gradient coupled with high residence time
450 of water in the estuary. Previous studies have showed that copper levels in the adjacent area to the
451 Tagus ($S \geq 30$) varied between 1.6 and 14.6, well below the values found at salinity 25 (Cotté-Krieff et al.,
452 2000; Santos-Echeandia et al., 2012). The correlation between Cu and L_1 ($r=0.67$, $p<0.05$) in the Tagus
453 estuarine waters suggest that the source of copper and ligands at mid-salinities is diluted at high
454 salinities. The inexistence of marshes downstream the inlet that connects the estuary to the sea
455 reinforces the hypothesis that salt marshes are the main source of copper and complexing ligands.
456 Moreover, the conditional stability constants for L_1 in the waters exported from the salt-marsh
457 (14.34 ± 0.27 for the non-colonized area and 14.17 ± 0.41 for the vegetated area) are comparable to the
458 ones present in the estuary (14.38 ± 0.37).

459 Although the conditional stability constants for L_2 in the waters derived from salt-marshes (12.12 ± 0.14
460 for the non-colonized area and 12.29 ± 0.46 for the vegetated area) are similar to those present in the
461 estuary, the input through tidal cycles is not reflected in the estuarine distribution of the weak ligand. As
462 shown before, L_2 concentrations decrease towards higher salinities. A photo-degradation process during
463 the transportation of these ligands to estuarine water with low particulate matter concentrations (5-15

464 mg L⁻¹ against 22-99 mg L⁻¹ for the Scheldt estuary, Zwolsman and van Eck., 1999) is a possible
465 explanation. The high residence time of the waters in the Tagus estuary would favor this degradation as
466 shown in the Scheldt estuary (Laglera and van den Berg., 2006). According to these authors L₂ is more
467 susceptible to photo-degradation than L₁, as the former is stabilized by its complexation with copper. In
468 addition, due to the heterogeneous distribution of this ligand, it is possible that several sources (i.e.
469 harbor, untreated effluents) contribute to the pool of weak ligands.

470 Considering the water volume of the Tagus estuary (1.9x10⁹ m³), the residence time during the sampling
471 conditions (60 days), the area covered by the intertidal non-vegetated zones (128 km²) and salt marshes
472 (20 km²) and the tidal induce transport of copper and ligands from the sediment to the water column in
473 the Rosário salt-marsh (Table 4), a contribution of around 7 nM of copper, 16 nM of L₁ and 52 nM of L₂
474 to the Tagus estuarine waters has been estimated. This account for 35% of Cu, 94% of L₁ and 45% of L₂
475 present in the estuary (S≥6).

476 This continuous input of copper complexing ligands is beneficial for the health of the estuary. Several
477 inputs of copper coming from a variety of sources, especially in such an industrialized and populated
478 area as it is the Tagus estuary can be neutralized by its binding to natural ligands. This would decrease
479 its toxicity to living organisms when an extra input of copper occurs (Louis et al., 2009).

480 **5. CONCLUSIONS**

481 Tagus estuarine waters show a relatively constant copper concentration during the estuarine mixing.
482 Most of this copper is organically complexed by a strong ligand (L₁) all through the estuary. A second and
483 weakest ligand (L₂) was also detected in these waters in higher concentrations. Salt-marsh areas are the
484 major sources of copper complexing ligands to the Tagus estuary. Noticeable, tidal induced transport
485 continuously feed estuarine waters with copper and ligands, mainly with the strongest one. Its input can
486 represent 95% of the ligand present in the estuary. Salt-marsh input of copper complexing ligands
487 determines copper distribution along the salinity gradient of the Tagus estuary.

488 Although future research should be performed to compare the importance of this source of ligands with
489 other sources like urban effluents, rivers or benthic inputs, the present work has demonstrated that salt
490 marsh areas are the main inputs of copper complexing ligands to the Tagus estuary.

491 This type of fluxes should be taken into account when assessing trace metal contamination problems
492 and remediation in estuarine and coastal areas. Furthermore, one may speculate that inundation of
493 coastal areas associated with the climatic changes, either to increase of water levels or floods will result
494 in additional fluxes of trace elements and copper complexing ligands from inter-tidal areas to estuarine
495 and coastal waters. The relevance of the tidal induced transport on copper and complexing ligands
496 coming from salt marsh areas may be crucial to understand the biogeochemical cycles of metals in
497 coastal ecosystems all over the world where salt-marshes occupy large extensions.

498

499 **Acknowledgements.** The authors would like to thank Vasco, Rute and Antonio for their kind sampling
500 cooperation during the sampling campaign. The C.S.I.C., under the program JAE-Doc (*Junta para la*
501 *Ampliación de Estudios*) co-funded by the *European Social Fund* (ESF), is greatly acknowledged for the
502 post-doctoral contract to J. Santos-Echeandía.

503 REFERENCES

- 504 - Biscombe., 2004. Factors influencing the seawater solubility of aerosol associated trace metals. PhD
505 Thesis. University of Plymouth.
- 506 - Braunschweig, F., Martins, F., Chambel, P., Neves, R., 2003. A methodology to estimate renewal time
507 scales in estuaries: the Tagus Estuary case. *Ocean Dynamics* 53, 137-145.
- 508 - Bruland, K.W., Donat, J.R., Hutchins, D.A., 1991. Interactive influences of bioactive trace metals on
509 biological production in oceanic waters. *Limnology and Oceanography* 36, 1555-1577.
- 510 - Buck, K., Bruland, K., 2005. Copper speciation in San Francisco Bay: a novel approach using multiple
511 analytical windows. *Marine Chemistry* 96, 185-198.
- 512 - Caçador, I., Costa, A., Vale, C., 2004. Carbon Storage in Tagus Salt Marsh Sediments. *Water Air Soil*
513 *Pollution: Focus* 4, 701-714.
- 514 - Caçador, I., Vale, C., Catarino, F., 1993. In: Vernet, J.-P. (Ed.), *Environmental contamination. Studies in*
515 *Environmental Science* vol. 55. Elsevier, Amsterdam, pp. 355-365.

- 516 - Caetano, M., Fonseca, N., Cesário, R., Vale, C., 2007. Mobility of Pb in salt marshes recorded by total
517 content and stable isotopic signature *Science of the Total Environment* 380, 84-92.
- 518 - Campos, M.L.A.M. and van den Berg, C.M.G., 1994. Determination of copper complexation in sea
519 water by cathodic stripping voltammetry and ligand competition with salicylaldoxime *Analytica*
520 *Chimica Acta* 284, 481-496.
- 521 - Chapman, C.S., Capodaglio, G., Turetta, C., van den Berg, C.M.G., 2009. Benthic fluxes of copper,
522 complexing ligands and thiol compounds in shallow lagoon waters. *Marine Environmental*
523 *Research* 67, 17-24.
- 524 - Cotté-Krieff, M.H., Guieu, C., Thomas, A.J., Martin, J.M., 2000. Sources of Cd, Cu, Ni and Zn in
525 Portuguese coastal waters. *Marine Chemistry* 71 (3-4), 199-214.
- 526 - Crespo, R., 1993. Cartografia do habitat potencial de passeriformes no Estuário do Tejo por
527 processamento digital de imagem. Degree Thesis. Faculdade de Ciências — Universidade de
528 Lisboa, Portugal, pp. 124.
- 529 - Croot, P.L., Moffet, J.W., Brand, L.E., 2000. Production of extracellular Cu complexing ligands by
530 eucaryotic phytoplankton in response to Cu stress. *Limnology and Oceanography* 45, 619-627.
- 531 - Gerringa, L.J., Herman, P.M., Poortvliet, T.C., 1995. Comparison of the linear Van den Berg/Ruzic
532 transformation and a non-linear fit of the Langmuir isotherm applied to Cu speciation data in the
533 estuarine environment. *Marine Chemistry* 48, 131-142.
- 534 - Gordon, A.S., Donat, J.R., Kango, R.A., Dyer, B.J., Stuart, L.M., 2000. Dissolved copper-complexing
535 ligands in cultures of marine bacteria and estuarine water. *Marine Chemistry* 70, 149-160.
- 536 - Kogut, M.B., Voelker, B.M., 2001. Strong copper-binding behavior of terrestrial humic substances in
537 seawater. *Environmental Science and Technology* 35, 1149-1156.
- 538 - Laglera-Baquer, L.M., González-Dávila, M., Santana-Casiano, J.M., 2001. Determination of metallic
539 complexing capacities of the dissolved organic material in seawater. *Scientia Marina* 65, 33-40.

- 540 - Laglera, L.M., van den Berg, C.M.G., 2003. Copper complexation by thiol compounds in estuarine
541 waters. *Marine Chemistry* 82 (1–2), 71–89.
- 542 - Laglera, L.M., van den Berg, C.M.G., 2006. Photochemical oxidation of thiols and copper complexing
543 ligands in estuarine waters. *Marine Chemistry* 101 (1–2), 130-140.
- 544 - Laglera, L.M., van den Berg, C.M.G., 2009. Evidence for geochemical control of iron by humic
545 substances in seawater. *Limnology and oceanography* 54, 610-619.
- 546 - Laglera, L.M., Downes, J., Santos-Echeandia, J., 2012. Comparison and combined use of non-linear
547 fitting for the estimation of complexing parameters from metal titrations of estuarine samples.
548 *Analytica Chimica Acta*, *submitted*.
- 549 - Leal, M.F.C., Vasconcelos, M.T.S.D., van den Berg, C.M.G., 1999. Copper induced release of complexing
550 ligands similar to thiols by *Emiliania huxleyi* in seawater cultures. *Limnology and Oceanography*
551 44, 1750-1762.
- 552 - Louis, Y., Garnier, C., Lenoble, V., Mounier, S., Cukrov, N., Omanovic, D., Pizeta, I., 2009. Kinetic and
553 equilibrium studies of copper-dissolved organic matter complexation in water column of the
554 stratified Krka River estuary (Croatia). *Marine Chemistry* 114, 110-119.
- 555 - Loureiro, J.M., 1979. Curvas de duração dos caudais medios diarios no rio Tejo. Technical Report,
556 Servico Hidraulico (DGRAH), Lisbon (1979).
- 557 - Mota, A.M., Cruz, P., Vilhena, C., Goncalves, M.L.S., 2005. Influence of the sediment on lead speciation
558 in the Tagus Estuary. *Water Research* 39, 1451-1460.
- 559 - Mucha , A.P., Almeida, C.M.R., Bordalo, A.A., Vasconcelos, M.T.S.D., 2010. LMWOA (low molecular
560 weight organic acid) exudation by salt marsh plants: Natural variation and response to Cu
561 contamination Estuarine, Coastal and Shelf Science 88, 63-70.
- 562 - Mucha , A.P., Almeida, C.M.R., Bordalo, A.A., Vasconcelos, M.T.S.D., 2008. Salt marsh plants (*Juncus*
563 *maritimus* and *Scirpus maritimus*) as sources of strong complexing ligands Estuarine, Coastal and
564 Shelf Science 77, 104-112.

- 565 - Pereira, P., Caçador, I., Vale, C., Caetano, M., Costa, A., 2007. Decomposition of belowground litter and
566 metal dynamics in salt marshes (Tagus Estuary, Portugal) *Science of the Total Environment* 380,
567 93-101.
- 568 - Pohl, C., Löffler, A., Hennings, U., 2004. A sediment trap flux study for trace metals under seasonal
569 aspects in the stratified Baltic Sea (Gotland Basin; 57°19.20' N; 20°03.00' E). *Marine Chemistry*
570 84, 143-160.
- 571 - Plavsic, M., Kwokal, Z., Strmecki, S., Peharec, Z., Omanovic, D., Branica, M. Determination of the copper
572 complexing ligands in the Krka rivers estuary. *Fresenius Environmental Bulletin* 18(3), 327-334.
- 573 - Quevauviller, P., Rauret, G., Rubio, R., Lopez-Sanchez, J.F., Ure, A., Bacon, J., Muntau, H., 1997.
574 Certified reference materials for the quality control of EDTA- and acetic acid-extractable contents
575 of trace elements in sewage sludge amended soils (CRMs 483 and 484). *Fresenius Journal of*
576 *Analytical Chemistry* 357, 611-618.
- 577 - Ruzic, I., 1982. Theoretical aspects of the direct titration of natural waters and its information yield for
578 trace metal speciation. *Analytica Chimica Acta* 140, 99-113.
- 579 - Santos-Echeandía, J., Laglera, L.M., Prego, R., van den Berg, C.M.G., 2008. Copper speciation in
580 estuarine waters by forward and reverse titrations. *Marine Chemistry* 108 (3-4), 148-158.
- 581 - Santos-Echeandía, J., Laglera, L.M., Prego, R., van den Berg, C.M.G., 2008. Dissolved copper speciation
582 behaviour during estuarine mixing in the San Simon Inlet (wet season, Galicia). Influence of
583 particulate matter. *Estuarine Coastal and Shelf Science* 76, 447-453.
- 584 - Santos-Echeandía, J., Prego, R., Cobelo-García, A., Millward, G.E., 2009. Porewater geochemistry in a
585 Galician Ria (NW Iberian Peninsula): implications for benthic fluxes of dissolved trace elements
586 (Co, Cu, Ni, Pb, V, Zn). *Marine Chemistry* 117, 77-87.
- 587 - Santos-Echeandía, J., Vale, C., Caetano, M., Pereira, P., Prego, R., 2010. Effect of tidal flooding on
588 metal distribution in pore waters of marsh sediments and its transport to water column (Tagus
589 estuary, Portugal) *Marine Environmental Research* 70, 358-367.

- 590 - Santos-Echeandía, J., Caetano, M., Brito, P., Canario, J., Vale, C., 2012. The relevance of defining trace
591 metal baselines in coastal waters at a regional scale: The case of the Portuguese coast (SW
592 Europe). *Marine Environmental Research*, in press.
- 593 - Shank, G.C., Skrabal, S.A., Whitehead, R.F., Kieber, R.J., 2004a. Strong copper complexation in an
594 organic-rich estuary: the importance of allochthonous dissolved organic matter. *Marine*
595 *Chemistry* 88, 21-39.
- 596 - Shank, G.C., Skrabal, S.A., Whitehead, R.F., Kieber, R.J., 2004b. Fluxes of strong Cu-complexing ligands
597 from sediments of an organic-rich estuary. *Estuarine Coastal and Shelf Science* 60 (2): 349-358.
- 598 - Skrabal, S.A., Donat, J.R., Burdige, D.J., 1997. Fluxes of copper-complexing ligands from estuarine
599 sediments. *Limnology and Oceanography* 42, 992-996.
- 600 - Skrabal, S.A., Donat, J.R., Burdige, D.J., 2000. Pore water distributions of dissolved copper and copper-
601 complexing ligands in estuarine and coastal marine sediments. *Geochimica et Cosmochimica Acta*
602 64, 1843-1857.
- 603 - Sundby, B., Vale, C., Caçador, I., Catarino, F., Madureira, M., Caetano, M., 1998. Metal-rich concretions
604 on the roots of salt marsh plants: Mechanism and rate of formation. *Limnology and*
605 *Oceanography* 43, 245-252.
- 606 - Turoczy, N.J., Sherwood, J.E., 1997. Modification of the van den Berg/ Ruzic method for the
607 investigation of complexation parameters of natural waters. *Analytica Chimica Acta* 354 (1-3),
608 15-21.
- 609 - Van den Berg, C.M.G., 1982. Determination of copper complexation with natural organic ligands in
610 seawater by equilibration with MnO₂ I. Theory. *Marine Chemistry* 11 (4), 307-322.
- 611 - Van den Berg, C.M.G. and Donat, J., 1992. Determination and data evaluation of copper complexation
612 by organic ligands in sea water using cathodic stripping voltammetry at varying detection
613 windows. *Analytica Chimica Acta* 257 (2), 281-291.

614 - Windom, H.L., Schropp, S.J., Calder, F.D., Ryan, J.D., Smith, R.G., Burney, L.C., Lewis, F.G., Rawlinson,
615 C.H., 1989. Natural trace metal concentrations in estuarine and coastal marine sediments of the
616 southeastern United States. *Environ. Sci. Technol.* 23, 314-320.

617 - Zwolsman, J.J.G., van Eck, G.T.M., 1999. Geochemistry of major elements and trace metals in
618 suspended matter of the Scheldt estuary, southwest Netherlands.
619 *Marine Chemistry* 66 (1-2), 91-111.

Figure captions.

Figure 1. Map of the Tagus estuary with the estuarine sampling stations and the Rosário salt-marsh (a) and schematic illustration of the sampling procedure in the salt-marsh

Figure 2. Dissolved copper and copper complexing ligands distribution during the Tagus estuarine mixing (a) 5 μM SA and (b) 10 μM SA detection windows. **Values presented are the mean of three replicates.**

Figure 3. Time course evolution of (a) copper and total ligand concentrations in the non-vegetated area (SP) and in the colonized area (CP) for the 5 μM detection window, (b) strong (L_1) and weak (L_2) ligand for the 5 μM detection window and (c) ligands (total, strong and weak) for the 10 μM detection window in flooding waters. **Values presented are the mean of three replicates.**

Supplementary material

Figure S1. Suspended particulate matter levels (a), particulate copper and aluminium concentrations (b), and labile copper concentrations (c) in the Tagus estuarine waters. **Values presented are the mean of three replicates.**

Figure S2. Ligand to copper ratios for the total ligand (L) and strong ligand (L_1) along the salinity gradient of the Tagus estuary.

Figure S3. (a) Low to high detection window ratios for the strong (L_1) and weak (L_2) ligand in the Tagus estuarine waters. (b) High to low detection window ratios for the strong (L_1) and weak (L_2) conditional stability constants.

Figure

[Click here to download high resolution image](#)

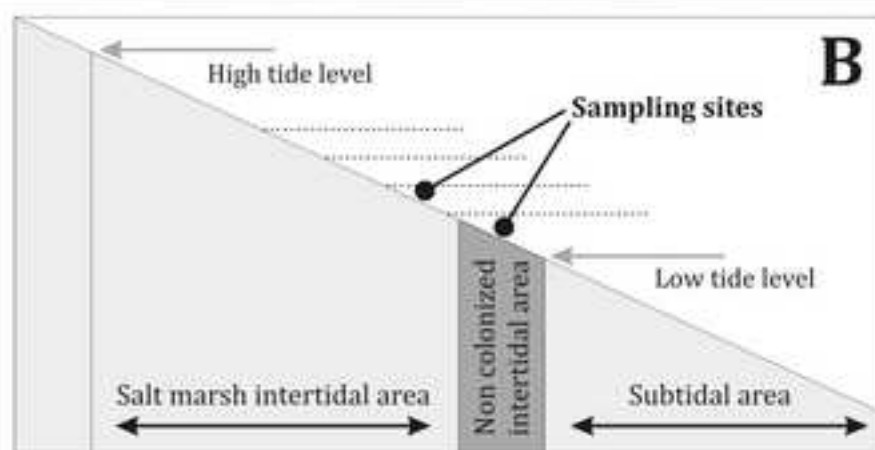
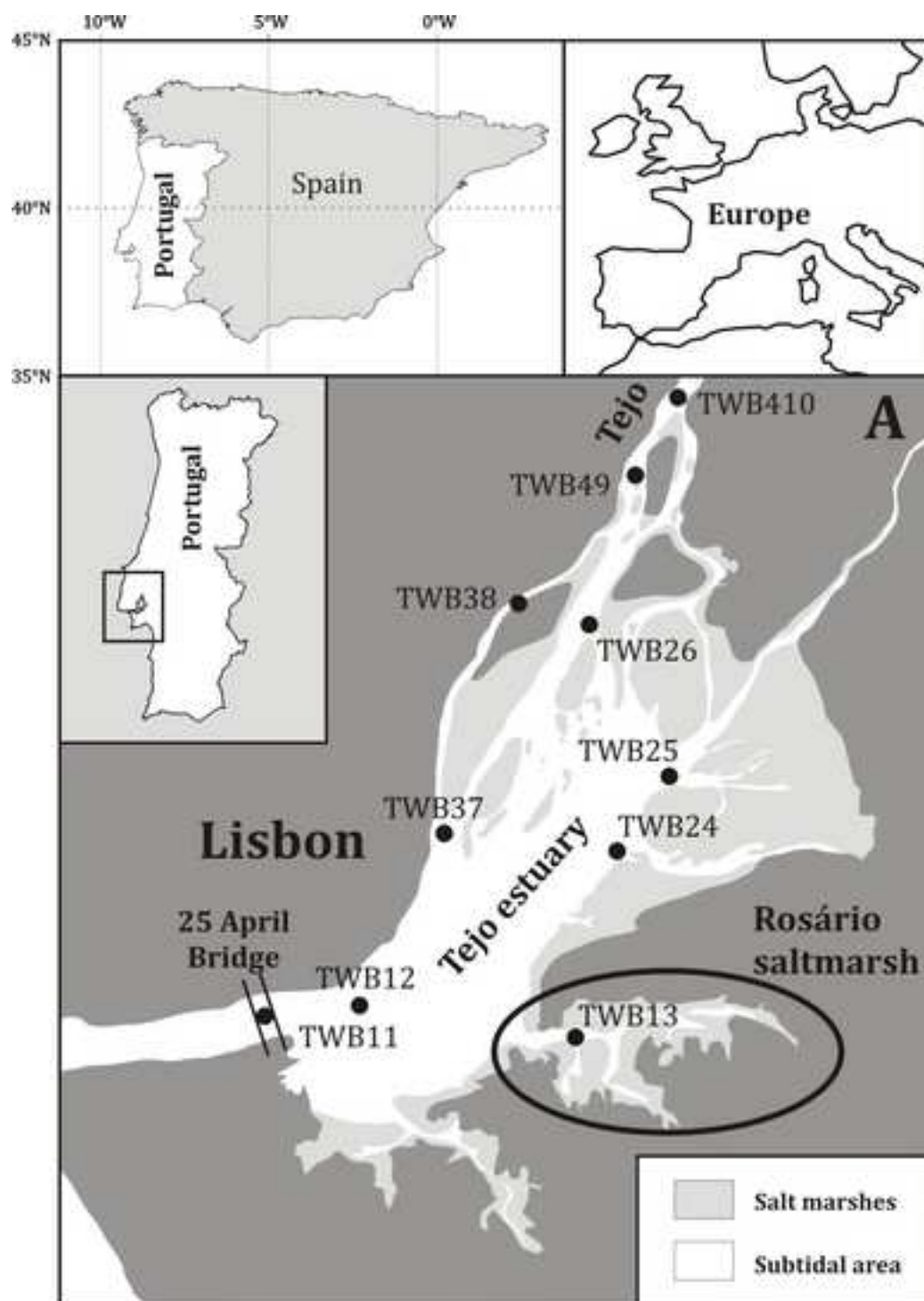
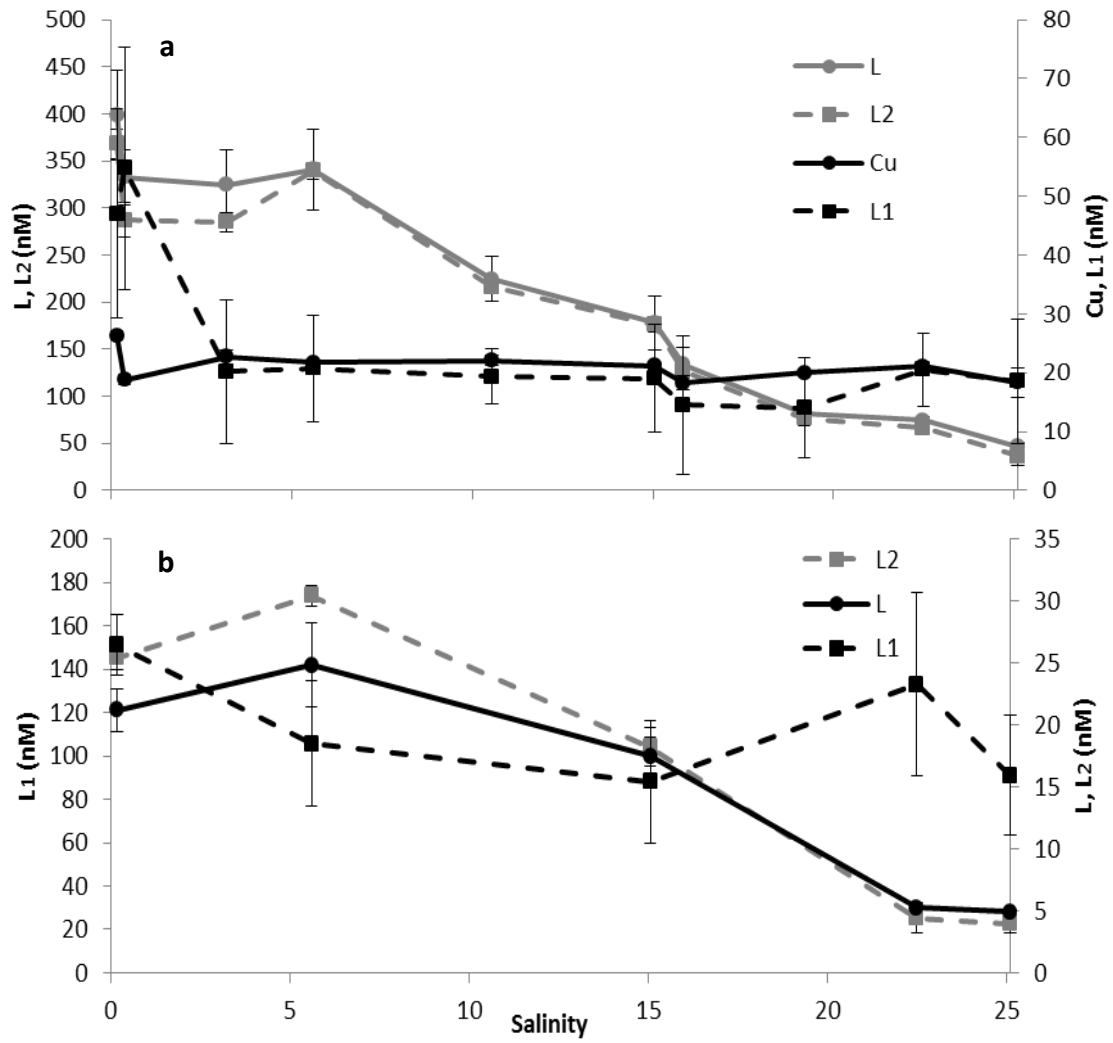


Figure 2.



Figure

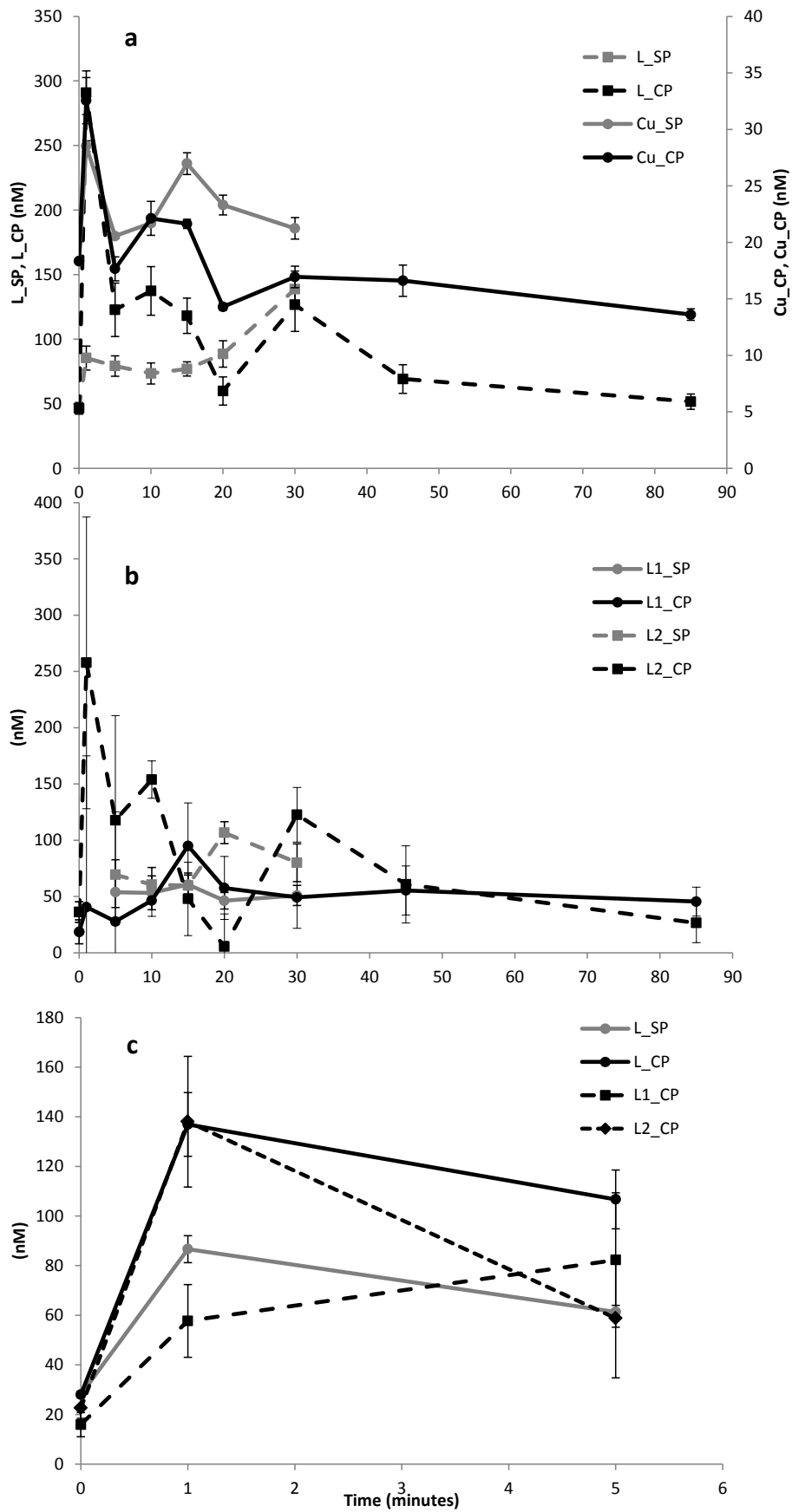


Figure 3.

Table 1. Dissolved ligand concentrations (nM) and conditional stability constants at two different detection windows (5 μ M SA and 10 μ M SA) in the Tagus estuarine waters. * sample 11, non linear fitting underestimated S, S^{INT} was used. Values underlined were obtained from an iterative linear fitting and used to obtain the rest of the parameters by nonlinear fitting. **Values presented are the mean of three replicates.**

Station	Salinity	5 μ M SA						10 μ M SA					
		L (nM)	Log K'	L ₁ (nM)	Log K ₁ '	L ₂ (nM)	Log K ₂ '	L (nM)	Log K'	L ₁ (nM)	Log K ₁ '	L ₂ (nM)	Log K ₂ '
TWB 410	0.2	399±48	13.15±0.11	47.0±17.8	15.09±0.09	368±16	12.96±0.09	121±10	14.52±0.11	26.4±2.5	16.84±0.50	145±6	13.87±0.05
TWB 49	0.4	333±30	13.26±0.09	54.8±20.6	15.10±0.35	287±19	13.13±0.10						
TWB 38	3.2	325±37	12.45±0.07	20.2±12.3	15.75±1.53	285±11	12.38±0.08						
TWB 26	5.6	341±43	12.21±0.06	20.7±9.0	<u>14.16±0.41</u>	339±9	12.08±0.06	142±19	13.13±0.11	18.5±5.1	<u>15.02±0.44</u>	174±5	12.76±0.05
TWB 37	10.5	225±24	12.25±0.08	19.4±4.7	<u>14.79±0.54</u>	217±5	12.09±0.04						
TWB 25	15.1	178±29	12.26±0.11	19.0±9.2	<u>14.10±0.46</u>	176±8	12.06±0.10	100±9	13.11±0.09	<u>15.4±5.0</u>	<u>14.71±0.37</u>	104±9	<u>12.76±0.10</u>
TWB 24	15.8	134±18	12.27±0.12	14.5±11.8	<u>14.14±0.71</u>	126±10	12.08±0.16						
TWB 12	19.2	82.4±5.5	12.75±0.08	14.0±8.5	<u>14.86±1.14</u>	76.9±7.5	12.37±0.16						
TWB 11*	22.5	74.6±4.0	12.93±0.11	20.6±6.2	<u>14.37±0.42</u>	66.5±5.4	12.29±0.19	30.0±2.2	14.15±0.19	23.3±7.4	14.59±0.45	25.1±6.5	12.50±0.34
TWB 13	25.1	46.5±4.3	13.11±0.13	18.6±10.6	<u>14.14±0.43</u>	36.2±9.2	12.42±0.59	28.0±1.3	13.76±0.07	15.9±4.9	<u>14.56±0.41</u>	22.6±4.2	12.76±0.27

Table 2. Dissolved ligand concentrations and conditional stability constants at two different detection windows (5 μM SA and 10 μM SA) in the flooding waters for the non-vegetated and vegetated areas of the Rosário salt-marsh. **Values presented are the mean of three replicates.**

Time (minutes)	Non-vegetated area						Vegetated area					
	<i>5μM SA</i>						<i>5μM SA</i>					
	L (nM)	Log K'	L ₁ (nM)	Log K ₁ '	L ₂ (nM)	Log K ₂ '	L (nM)	Log K'	L ₁ (nM)	Log K ₁ '	L ₂ (nM)	Log K ₂ '
0	46.5±4.4	13.11±0.10	18.6±10.6	14.00±0.43	36.2±9.2	12.42±0.59	46.5±4.4	13.11±0.10	18.6±11	14.00±0.43	36.2±9.2	12.42±0.59
1	85.4±9.3	14.04±0.26					291±17	13.11±0.09	40.5±134	14.08±0.81	258±130	12.91±0.27
5	79.2±7.9	13.73±0.19	53.8±13.6	14.17±0.52	69.3±13.3	12.18±0.29	123±21	13.55±0.63	27.7±97	14.83±1.13	118±93	13.05±0.50
10	73.5±8.1	13.94±0.25	53.2±15.0	14.32±0.79	60.6±15.2	12.22±0.35	137±19	13.22±0.26	46.5±14	14.71±0.36	154±17	12.27±0.18
15	77.0±5.5	13.84±0.13	60.6±8.5	14.12±0.24	59.7±11.2	12.01±0.26	118±14	13.40±0.19	95.0±38	13.61±0.25	47.9±33	11.96±0.62
20	88.6±10.3	13.77±0.26	46.3±7.4	14.79±0.54	107±9.8	12.26±0.16	59.9±11	13.88±0.63	57.6±28	13.92±0.36	5.5±29	11.96±1.38
30	139±14	13.91±0.23	50.9±8.9	14.31±0.41	70.1±16.8	11.95±0.25	127±21	13.22±5.13	49.2±28	14.14±0.39	123±24	12.30±0.31
45							69.2±11	13.76±5.15	55.4±22	14.00±0.33	60.8±34	11.87±0.50
85							51.7±5.9	13.89±5.07	45.5±13	14.03±0.25	26.5±18	11.99±0.59
							<i>10μM SA</i>					
0	28.0±1.3	13.76±0.07	15.9±4.9	14.56±0.41	22.6±4.2	12.76±0.27	28.0±1.3	13.76±0.07	15.9±4.9	14.56±0.41	22.6±4.2	12.76±0.27
1	86.7±5.4	14.48±0.10					137±13	14.47±0.17	57.7±15	15.69±0.39	138±26	13.44±0.21
5	61.4±2.6	14.39±0.06					107±12	14.32±0.20	82.3±27	14.63±0.26	58.8±24	12.84±0.49

Table

[Click here to download Table: Table_3.doc](#)

Table 3. Dissolved copper and ligand concentrations and conditional stability constants at two different detection windows (5 $\mu\text{M SA}$ and 10 $\mu\text{M SA}$) in the porewaters of the Rosário salt-marsh for the non-vegetated and vegetated areas. **Values presented are the mean of three replicates.**

ROSARIO SALT-MARSH (5 $\mu\text{M SA}$)														
Non-vegetated area								Vegetated area						
Depth (cm)	Cu (nM)	L (nM)	Log K'	L ₁ (nM)	Log K ₁ '	L ₂	Log K ₂ '	Cu (nM)	L (nM)	Log K'	L ₁ (nM)	Log K ₁ '	L ₂	Log K ₂ '
2	53.9±5.4	245±32	13.58±0.28	184±24	13.70±1.03	70.1±24	13.09±1.42	142±8	831±80	13.55±0.19	203±187	15.17±0.82	666±176	13.09±0.27
6	45.3±1.0	321±34	13.24±0.17	77.2±43	14.77±0.58	287±39	12.68±0.21	70.7±2.0	767±36	12.88±0.07	115±61	14.66±0.44	699±57	12.82±0.10
ROSARIO SALT-MARSH (10 $\mu\text{M SA}$)														
Non-vegetated área								Vegetated área						
2	53.9±5.4	230±18	14.28±0.10	66.8±94	15.25±0.71	182±89	13.85±0.29	142±8	419±13	13.95±0.14	148±55	17.56±2.44	846±65	13.51±0.22

Table 4. Estimated tidal induced transport of dissolved copper and complexing ligands in Rosário sediments for the non-vegetated and colonized areas.

		Tidal induced transport ($\mu\text{mol m}^{-2} \text{d}^{-1}$)	
		Non-vegetated	Colonized
5 μM SA	Cu	1.23	2.43
	L	3.25	48.2
	L ₁	2.16	11.5
	L ₂	2.31	64.7
10 μM SA	L	4.25	6.87
	L ₁	-	3.80
	L ₂	-	5.77

Electronic Supplementary Material (online publication only)

[Click here to download Electronic Supplementary Material \(online publication only\): Figure_S1.docx](#)

Electronic Supplementary Material (online publication only)

[Click here to download Electronic Supplementary Material \(online publication only\): Figure_S2.docx](#)

Electronic Supplementary Material (online publication only)

[Click here to download Electronic Supplementary Material \(online publication only\): Figure_S3.docx](#)